ATTENTION MICROFICHE USER,

The original document from which this microfiche was made was found to contain some imperfection or imperfections that reduce full comprehension os some of the text despite the good technical quality of the microfiche itself. The imperfections may be:

- missing or illegible pages/figures;
- wrong pagination;
- poor overall printing quality, etc...

We normally refuse to microfiche such a document and request a replacement document (or page) from the national INIS Centre concerned. However, our experience shows that many months pass before such documents are replaced. Sometimes the Centre is not able to supply a better copy or, in some cases, the pages that were supposed to be missing correspond to a wrong pagination only. We feel that it is better to proceed with distributing the microfiche made of these documents than to withold them till the imperfections are removed. If the removals are subsequestly made then replacement microfiche can be issued. In line with this approach then, our specific practice for microfiching documents with imperfections is as follows:

1. A microfiche of an imperfect document will be marked with a special symbol (black circle) on the left of the title. This symbol will appear on all masters and copies of the document (1st fiche and trailer fiches) even if the imperfection is on one fiche of the report only.

2. If imperfection is not too general the reason will be specified on a sheet such as this, in the space below.

3. The microfiche will be considered as temporary, but sold at the normal price. Replacements, if they can be issued, will be available for puchase at the regular price.

4. A new document will be requested from the supplying Centre.

5. If the Centre can supply the necessary pages/document a new master fiche will be made to permit production of any replacement microfiche that may be required.

The original document from which this microfiche has been prepared has these imperfections:

MISSING: ~~pages~~/figures numbered: 3

wrong pagination

poor overall printing quality : Illegible printing -

combinations of the above

INIS CLEARINGHOUSE
IAEA
P.O. Box 100
A-1400, Vienna-AUSTRIA

IAEA-NDS- 95
Rev. 0

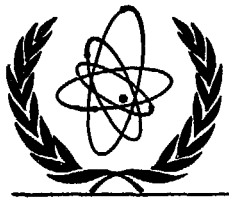

INTERNATIONAL ATOMIC ENERGY AGENCY

NUCLEAR DATA SERVICES

DOCUMENTATION SERIES OF THE IAEA NUCLEAR DATA SECTION

EMPIRE

Pre-equilibrium/Compound Nuclear Model Code for Personal Computer

A. Marcinkowski
Institute of Nuclear Studies
Warsaw, Poland

Abstract: The pre-equilibrium/compound nuclear model code EMPIRE was implemented for use on personal computer. It is available on a set of diskettes from the NEA Data Bank of Nuclear Energy Agency (Saclay, France) and the IAEA Nuclear Data Section.

Implemented on PC by
V. Goulo

May 1988

EMPIRE

Pre-equilibrium/Compound Nuclear Model Code for Personal Computer

Introduction

Code EMPIRE [1,2] is based on the statistical compound model and the pre-equilibrium hybrid or multistep compound emission model. It has been written with angular momentum conservation taken into account throughout the whole calculations.

It was presented at the Workshop on Applied Nuclear Theory and Nuclear Model Calculations for Nuclear Technology Applications in the International Centre for Theoretical Physics, Trieste (15 February - 18 March 1988). It has been implemented for IBM compatible personal computers Olivetti M-24 and M-380, using professional FORTRAN compiler [3].

1. Changes in the text program

Originally, EMPIRE code has been written for CDC 6600 computer on FORTRAN IY programming languange. To be implemented on IBM personal computer, the following modifications were made:

a. Input/output operators were written according to FORTRAN Reference Manual [4].

b. Work with scratch files was re-organized in unformatted mode in consistent way.

c. Subroutines BRE and BWR were changed making them without ENTRY point and EOF procedure.

d. Subroutine ILOW of multicascade calculation organization was changed for reading of gamma transitions of previous step reaction.

2. Compiling and linking of the code was done in accordance with PROFORT 1.0 compiler manual [2], using compilers library of standard subroutines.

3. Example of batch file

```
EMP /R 60000 >EMP2.LST <EMP2.INP

where EMP is an execution module of the code
      EMP2.INP is input data file
      EMP2.LST is output listing
```

4. Examples of input/output data files used in exercises are described in the proceedings of the Workshop and are available together with the source file of the code on a diskette.

5. Running time of the exercises: 15-20 minutes for 16 Mhz computer.

References

1. M. HERMAN, A. MARCINKOWSKI, K. STANKEVICH, A Program for Calculation of Spectra and Cross Sections Within the Combined Pre-equilibrium/ Compound Nucleus Model of Nuclear Reactions. Computer Physics Communications 33(1984)373-398.

2. A. MARCINKOWSKI, EMPIRE - A Program for Calculation of Spectra and Cross Sections Within the Combined Pre-equilibrium/Compound Nucleus Model of Nuclear Reactions. To be published in the proceedings of the Workshop.

3. Professional FORTRAN Reference Manual, 1986.

4. Professional FORTRAN Compiler. Installation and use, 1984.

EMPIRE - A Program for Calculation of Spectra and Cross Sections within the Combined Pre-equilibrium/Compound Nucleus Model of Nuclear Reactions

A. Marcinkowski
Institute for Nuclear Studies, Warsaw, Poland

Abstract

A computer code based on the statistical compound nucleus model and the pre-equilibrium hybrid model or the multi-step compound emission model is described. Angular momentum conservation is observed throughout the whole calculation. The models, the structure of the code and the content of input and output are described. The validation of the calculations by comparison with experimental data for some neutron induced reactions is also presented.

1. Nature of the physical problem

The code EMPIRE is designed for calculation of essential characteristics of a large variety of nuclear reactions involving light particles and gamma-rays. The program is flexible enough to treat capture cross sections at energies below 1 MeV, as well as successive multiparticle emission at energies of several tens of MeV. These features enable a consistent treatment of all competitive channels, which contribute significantly to the reaction cross section, within a single computer run, and impose high constraints on the parameterization of the models involved. This possibility has proved advantageous in many reaction mechanism studies and evaluation applications [1,2].

The energy-averaged cross sections for reactions with several emitted particles and gamma-rays, under the assumption of sequential evaporation, are evaluated according to the different ways, in which a particular state of a final nucleus by such a reaction can be reached, as illustrated in fig. 1. Each evaporation ster is treated in the framework of the statistical theory of the compound nucleus (CN). In the first stage of the reaction the pre-equilibrium emission of neutrons and protons is calculated, i.e. the multiple pre-equilibrium decay, simultaneous or sequential and the emission of complex particles are disregarded. The multiparticle pre-equilibrium decay appears to play some role at projectile energies approaching 50 MeV and becomes increasingly significant at higher excitations [3]. The pre-equilibrium decay dominates the alpha-particle emission for heavy nuclei, where this channel is rather unsignificant because of the Coulomb barrier effects. Nevertheless these omissions put natural limitations on the applicability of the calculations. Another constraint is imposed by omission of the fission channel, which limits the applicability of the code to nonfissionable nuclei.

The parity and angular momentum conservation are observed throughout the entire calculations. To this end angular momentum

considerations have been incorporated into the geometry dependent hybrid (GDH) model [4], describing the emission of nucleons prior to the equilibration of the excited nucleus. This model has been choosen for calculation of the a priori pre-equilibrium cross sections, for it provides a better description of the physical process, i.e. a higher probability of peripheral collisions to undergo pre-equilibrium decay than for central collisions. It offers also the attractive possibility of avoiding the use of free parameters by assuming the option for evaluation of the nucleon mean free path in the nucleus from the absorptive imaginary optical potential.

Another option in the newest version of EMPIRE is the calculation of the pre-equilibrium emission yields for nucleons, quantum-mechanically, according to the theory of Feshbach, Kerman and Koonin [5] for the multi-step compound (MSC) decay. The MSC emission accounts for that portion of the pre-equilibrium emission, which is due to the decay of bound-particle configurations forming the chain of doorway states developing towards increasing complexity. It is responsible forthe symmetric portion of the angular distribution only and thus does not exhaust the full pre-equilibrium cross section, but in some situations it may play the dominant role [6].

The decay of the compound nucleus is treated either in terms of the HRTW theory [7,8], which redefines all the inelastic channels in order to account for the width fluctuations caused by the correlation of the incident and outgoing waves in the elastic channel, or in terms of the standard Hauser-Feshbach theory, at higher energies, where many open channels cause the effect of the width fluctuation to cancel. The former theory is of particular importance for calculation of the first chance gamma-rays at low neutron energies, close to the inelastic channel threshold.

The calculated a priori pre-equilibrium cross sections are used to rescale the magnitude of the compound nucleus cross sections so as to satisfy the normalization of their incoherent sum to the optical model reaction cross section.

The EMPIRE program is specially well suited for calculation of:

- activation cross sections,
- isomeric cross sections,
- production cross sections for gamma-rays accompanying the decay of low excited levels,
- energy spectra for emitted particles and gamma-rays.

The first three types of data are available, from the output, for final nuclei of each stage in the multi-particle emission. In addition the energy-spin distributions of population of states for the intermediate nuclei, for both parities, are given at each stage. Similarly the energy spectra of the reaction products in all assumed competing channels are given at the end for each stage.

The EMPIRE code has been published [9] and made available via the C.P.C. Program Library of the Queens University of Belfast. Since then it has been validated in many calculations of fast neutron cross section for structural materials, as well as for

lighter and heavy nuclei. The code has been included also in the International Nuclear Model Code Intercomparison, for Spherical Optical and Statistical Model Study, carried out by the NEA Data Bank under the auspices of the IAEA. The results of intercomparison have been widely discussed in ref. [10]. In fig. 2 one of the comparisons is shown.

The following charters contain the detailed description of the models and formalism employed in proceeding of the code, the methods of solutions and the structure of the code, the restrictions on the complexity of the problem imposed by the practicity of the digital calculations and eventually the comparison of calculations with experimental data is presented.

2. Models and formulation applied in the EMPIRE code

2.1 Formation and decay of the compound nucleus

2.1.1 The Hauser-Feshbach formula for compound nucleus cross section

The phenomenological reaction cross section for a projectile with a wavelength of the relative motion λ_a is usually written in terms of the partial wave transmission coefficients T_l^a of the optical model potential barrier

$$\sigma_R = \pi \lambda_a^2 \sum_{l=0}^{\infty} (2l+1) T_l^a \quad . \tag{1}$$

It coincides with the cross section for the formation of the CN in the limit of no pre-equilibrium emission. In case when the probability of particle emission $P_b^l(\varepsilon)$ prior to the formation of the CN is nonnegligible the cross section for the formation of the CN reads.

$$\sigma_{CN} = \pi \lambda_a^2 \sum_{l=0}^{\infty} (2l+1) T_l^a \left[1 - \sum_x \int_0^{E-B_x} P_x^l(\varepsilon) d\varepsilon \right], \tag{2}$$

where E is the excitation energy of the CN and B_x is the binding energy of the ejectile. Assuming the channel spin $\vec{S}=\vec{s}_T+\vec{s}_a$, with s_T, s_a being the spins of the target nucleus and of the projectile, and considering the formation of a CN state with definite spin $\vec{I}=\vec{S}+\vec{l}$ and parity π requires replacement of the summation over the orbital angular momentum l by a triple sum indicating the coupling of appropriate angular momenta

$$\sigma_{CN} = \pi \lambda_a^2 \sum_{I^\pi=0}^{\infty} \sum_{S=|s_T-s_a|}^{s_T+s_a} \sum_{l=|I-S|}^{I+S} g_I T_l^a \left[1 - \sum_x \int_0^{E-B_x} P_x^l(\varepsilon) d\varepsilon \right]. \tag{3}$$

In writing (3) use was made of the relation

$$\sum_{I=|S-l|}^{S+l} (2I+1) = (2l+1)(2S+1) \tag{3a}$$

and the usual notation $g_I=(2I+1)/(2s_a+1)(2s_T+1)$ for the statistical weighting factor was adopted.

The optical model offers the possibility to calculate the j-dependent transmission coefficients T_l^{ja}, use of which leads to a coupling scheme $\vec{j}_a=\vec{l}+\vec{s}_a$ and $\vec{I}=\vec{s}_T+\vec{j}_a$, reducing the summation over S and l to

$$\sum_{j_a=|I-S_T|}^{I+S_T} T_l^{j_a} = \sum_{l=|I-S_T|-S_a}^{I+S_T-S_a} T_l^{j_a=l+S_a} + \sum_{l=|I-S_T|+S_a}^{I+S_T+S_a} T_l^{j_a=l-S_a} \quad (4)$$

The resulting cross section is now

$$\sigma_{CN} = \pi\lambda_a^2 \sum_{I^\pi=0}^{\infty} \sum_{j_a=|I-S_T|}^{I+S_T} g_I T_l^{j_a} R^l, \quad (5)$$

with R^l being the reduction factor in square brackets of eq.(2), which accounts for the loss of flux due to pre-equilibrium (PE) emission.

The decay of the CN is calculated according to the Hauser-Feshbach formula, which factorizes into the formation cross section and the emission probability for an ejectile b

$$T_b / \sum_c T_c , \quad (5a)$$

leaving the residual nucleus with an excitation energy U_b in a state of spin I_b and parity π_b. The decay width Γ_b is governed by the densities of levels, which undergo the decay $\rho(U,I,\pi)$ and of those accessible, after emission, in the residual nucleus $\rho(U_b,I_b,\pi_b)$.

$$\Gamma_b(U,I,\pi) = \frac{1}{2\pi\rho(U,I,\pi)} \sum_{I^\pi=0}^{\infty} \int_0^{E-B_b} \sum_{j_b=|I-I_b|}^{I+I_b} T_l^{j_b} \rho(U_b,I_b,\pi_b)\, dE . \quad (6)$$

The cross section thus reads,

$$\frac{d\sigma(U_b,I_b,\pi_b)^{\pi F}}{dU_b} = \pi\lambda_a^2 \sum_{j_a=|I-S_T|}^{I+S_T} g_I T_l^{j_a} R^l \sum_{j_b=|I-I_b|}^{I+I_b} T_l^{j_b} \rho(U_b,I_b,\pi_b) / \sum_c T_c \quad (7)$$

where the summation, in the denominator, over all competing particles c being emitted assures proper normalization of the decay probability,

$$\sum_c T_c = \sum_c \sum_{I_c^\pi=0}^{\infty} \sum_{j_c=|I-I_c|}^{I+I_c} \int_0^{E-B_c} T_l^{j_c} \rho(U_c,I_c,\pi_c)\, dU_c . \quad (7a)$$

The parity selection rules are implicitely imposed on all the summations in eqs. (3) to (7a), as indicated by the index π. The reduction factor R is l or j dependent in accordance with the adopted PE emission model.

2.1.1 The width fluctuation effects at low neutron energies

The factorization of the CN cross section, in terms of the optical model transmission coefficients, as given by the Hauser Feshbach formula (7), is a good assumption when many channels are open. The factorization breaks however, thus violating the Bohr, s hypothesis, as a result of width fluctuation, at low energies when only few strongly and weakly absorbing channels are mixed. This case is of particular interest in applied work involving neutron capture or low energy neutron scattering. Even in this case the factorization of the cross section can be

reestablished by introducing the channel correction factors, which result in redefinition of the effective partial wave transmission coefficients V_{ℓ}^{ja} in the inelastic channels and the appearance of the enhancement factor W_{la}^{ja} in the elastic channell [8]. In the framework of the HRTW theory [8] the CN cross section factorizes in a way similar to eq. (7),

$$\frac{d\sigma(U_b,I_b,\pi_b)}{dU_b}^{HRTW} = \pi\lambda_a^2 \sum_{I^\pi=0}^{\infty} \sum_{j_a=|I-s_T|}^{I+s_T} g_I V_{la}^{ja} R^{\ell} \sum_{j_b=|I-I_b|}^{I+I_b} V_{\ell_b}^{j_b} \rho(U_b,I_b,\pi_b)\left[1+\delta_{a\ell_b}\delta_{j_a j_b}\delta_{\varepsilon_a\varepsilon_b}\delta_{ab}\left(W_{la}^{ja}-1\right)\right] \Big/ \sum_c V_c \quad (7b)$$

$$\text{with} \quad \sum_c V_c = \sum_c \sum_{I_c^\pi=0}^{\infty} \sum_{j_c=|I-I_c|}^{I+I_c} \int_0^{E-B_c} V_{\ell_c}^{j_c} \rho(U_c,I_c,\pi_c)\,dU_c \quad (7c)$$

The measure of the lack of unitarity of the average S-matrix, $T_a = 1 - |\langle S_{aa}\rangle|^2 \simeq \sum_b |\langle S_{ab}\rangle|^2$, provides the relation between the optical model transmission coefficients and V_{la}^{ja}

$$T_{\ell}^{ja} = V_{la}^{ja} + (V_{la}^{ja})^2 \left(\sum_c V_c\right)^{-1} \left(W_{la}^{ja}-1\right). \quad (8)$$

The elastic enhancement factor W_{la}^{ja} varies between 2 and 3 for strong and weak absorption, respectively. It has been also related to the transmission coefficients T_{ℓ}^{ja} by generating numerically the statistical S-matrix [11],

$$W_{la}^{ja} = 1 + \frac{2}{1+(T_{\ell}^{ja})^{\varkappa}} + (87\pm5)\left(\frac{T_{\ell}^{ja}-\bar{T}}{\sum_c T_c}\right)^2 \left(\frac{T_{\ell}^{ja}}{\sum_c T_c}\right)^5, \quad (9)$$

$$\text{where} \quad \varkappa = 4\,\frac{\bar{T}}{\sum_c T_c}\left(1+\frac{T_{\ell}^{ja}}{\sum_c T_c}\right)\Big/\left(1+3\,\frac{\bar{T}}{\sum_c T_c}\right) \quad \text{and} \quad \bar{T} = \frac{\sum_c T_c^2}{\sum_c T_c} \quad (10)$$

For a given elastic enhancement factor W_{la}^{ja} eq. (8) can be solved by iteration. Making use of the fact that $V_{la}^{ja}\left(\sum_c V_c\right)^{-1} \simeq T_{\ell}^{ja}\left(\sum_c T_c\right)^{-1}$ the first step iteration gives for V_{la}^{ja}

$$^{(1)}V_{la}^{ja} = T_{\ell}^{ja}\left[1+\frac{T_{\ell}^{ja}}{\sum_c T_c}\left(W_{la}^{ja}-1\right)\right]^{-1} \quad (11)$$

Already $^{(1)}V$ approaches the exact solution of eq. (8), when the number of open channels does exceed 20. If not we follow up to

$$^{(i+1)}V_{la}^{ja} = T_{\ell}^{ja}\left[1+\frac{^{(i)}V_{la}^{ja}}{\sum_c {}^{(i)}V_c}\left(W_{la}^{ja}-1\right)\right]^{-1}. \quad (12)$$

One can see from eq. (11) that for a large number of open channels even in the case of strong absorption ($T_{\ell}^{ja} \simeq 1$) $T_{\ell}^{ja} \ll \sum_c T_c$ and the Hauser-Feshbach formula holds.

2.1.3 The level densities

The level density $\rho(U,I,\pi) = \frac{1}{2}\rho(U,I)$ is calculated according to the two-component formula by Cameron and Gilbert [12]. In the region of high excitations the model predicts

$$\rho_H(U,I) = \frac{\sqrt{\pi}}{12}\,\frac{\exp[2\sqrt{a(U-\Delta)}]}{a^{1/4}(U-\Delta)^{5/4}}\,\frac{(2I+1)}{2\sqrt{2\pi}\sigma^3}\exp\left[-\frac{(I+\frac{1}{2})^2}{2\sigma^2}\right], \qquad (13)$$

with the level density parameter a and the pairing energy shift Δ. At excitation energies lower than the matching point U_x a constant temperature T approximation is assumed

$$\rho_L(U,I) = \frac{1}{T}\exp[(U-U_0)/T]\,\frac{(2I+1)}{2\sqrt{2\pi}\sigma^3}\exp\left[-\frac{(I+1/2)^2}{2\sigma^2}\right], \qquad (14)$$

where U_0 and the nuclear temperature T are free parameters related to the observed discrete levels. The requirement that the two formulae provide level densities, which are tangent at the matching energy U_x leads to the relations

$$U_0 = U_x - T(\ln T)\rho_H(U_x), \qquad (15)$$

$$T = \left[\sqrt{\frac{a}{U_x-\Delta}} - \frac{3}{2(U_x-\Delta)}\right]^{-1}. \qquad (16)$$

Once a and one of the parameters U_0, T, U_x are defined the remaining two parameters are calculated from eqs. (15) and (16). Two options for choosing the spin cut-off parameter σ^2 are available in EMPIRE. The Fermi gas model predicts

$$\sigma^2 = \frac{6}{\pi^2}\,k A^{2/3}\sqrt{a(U-\Delta)}, \qquad (17)$$

where $k A^{2/3} = \langle m^2 \rangle$ is an average taken over angular momentum projections m of single particle states in the vicinity of the Fermi energy. The value of the constant k has been evaluated by Cameron and Gilbert to be 0.146, while 0.24 was suggested by Reffo [13]. Alternative is the rigid-body formula

$$\sigma^2 = 1.505 \cdot 10^{-2} A^{5/3}\sqrt{(U-\Delta)/a}. \qquad (18)$$

In the low energy range, below U_x, the spin cut-off parameter is linearly interpolated between the value σ^2_{dl} calculated for the $N \geq 5$ known excited levels with spins I_i (ground state excluded),

$$\sigma^2_{dl} = \frac{1}{2N}\sum_{i=1}^{N}\left(I_i + \frac{1}{2}\right)^2, \qquad (19)$$

given by the maximum likelihood method, and the value of σ^2 from eqs. (17) or (18)

$$\sigma^2(U) = \frac{\sigma^2(U_x) - \sigma^2_{dl}}{U_x - U_{cut}}(U - U_{cut}) + \sigma^2_{dl}, \qquad (20)$$

where U_{cut} is the energy of the highest known level. At excitation energies lower than U_{cut} the discrete levels are counted

$$\varrho(U,I,\pi) = \sum_{i=1}^{N} \delta(U-U_i)\,\delta_{II_i}\,\delta_{\pi\pi_i}\,. \qquad (21)$$

The parameterization of the above given formulae may be found in the original paper of Cameron and Gilbert [12] or in the extensive elaboration by Reffo [13]. To allow the use of other models the program accepts also numerical level densities put in point-by-point for spin sequences from 1/2 to 59/2 or from 0 to 29 at twenty excitation energies 3, 6, 9.... 60 MeV. Level densities for particular nuclei should be placed in order, in which they appear in the main input.

2.1.4 Partial wave transmission coefficients for particles and transmission coefficients for gamma-rays

The j-dependent transmission coefficients for particles used throughout the calculations are computed from a spherical optical model (OM) by means of the subroutine SCAT [14]. A potential well is generated from the input parameters and the radial Schrödinger equation is solved for partial waves by numerical integration outwards the optical potential is negligible. At this point the radial wave function for each partial wave, being solution , is joint to its asymptotic value , using logarithmic derivative. This yields the phase shifts δ_{lj} or more precisely the average scattering matrix $\langle S_{ij}\rangle = \exp 2i\delta_{lj}$, which defines the transmission coefficients

$$T_l^j = 1 - |\langle S_{lj}\rangle|^2 \,. \qquad (22)$$

There are several potential well forms available in the program, which cover the range of those currently of interest. The general parameterization is of the following form

(23)

$$V_{OM}(r) = -V_V f(r,r_V) + V_{SO}\left(\frac{\hbar}{M_\pi c}\right)^2 \frac{1}{r}\left[\frac{d}{dr} f(r,r_{SO})\right]\vec{l}\cdot\vec{s} - i\left[W_V f(r,r_W) - 4W_S \frac{d}{dr} f(r,r_S)\right],$$

where $f(r,r_i) = \{1 + \exp(r-r_i A^{1/3})/a_i\}^{-1}$ is the Woods-Saxon form factor.
The surface, absorptive term with well depth W_S is sometimes assumed to have the Gaussian shape $f(r,r_S) = \exp-[(r-r_S A^{1/3})/a_S]^2$.
The existing global parameterizations of the OM use potential wells, which depend on the projectile energy in many ways. The EMPIRE code offers three most common options

$$\begin{aligned} V_i &= V_i(1), \\ V_i &= V_i(1) + V_i(2)\ln E_a, \\ V_i &= V_i(1) + V_i(2)E_a + V_i(3)E_a^2 \quad \text{and} \\ W_i &= W_i(1), \end{aligned} \qquad (24)$$

$$W_i = W_i(1) + W_i(2)\ln E_a,$$

$$W_i = W_i(1) + W_i(2)E_a + W_i(3)E_a^2 .$$

In addition some of the mostly used global OM potentials, namely the ones reported by Moldauer [15], Björklund and Fernbach [16], Becchetti and Greenless [17] and Wilmore and Hodgson [18], for neutrons, Björklund and Fernbach [16], Becchetti and Greenless [17], for protons and McFadden and Satchler [19] for alpha particles are included as separate options. Both the individual and/or the global OM potentials can be applied in defined energy intervals. Different potentials in different energy regions with practically unlimited number of energy regions.

The transmission coefficients for gamma-rays are calculated from the radiative strength functions

$$f_{X\ell} = \frac{\Gamma^I_{\gamma X\ell}}{E_\gamma^{2\ell+1} D_I} , \qquad (25)$$

in accordance with the known definition

$$T_\gamma^{X\ell} = 2\pi \frac{\Gamma^I_{\gamma X\ell}}{D_I} = 2\pi f_{X\ell} E_\gamma^{2\ell+1} . \qquad (26)$$

Here D_I denotes the spacing of levels with spin I and Xl stands for electric E or magnetic M transition of multipolarity l.

The Weisskopf single-particle model [20] prescribes the strength functions for electric transitions of multipolarity l

$$f_{E\ell} = \frac{18(\ell+1)}{\ell(\ell+3)^2[(2\ell+1)!!]^2} \frac{(2\ell+1)}{D_0} \frac{e^2}{\hbar c} \left(\frac{R}{\hbar c}\right)^{2\ell} \qquad (27)$$

and for magnetic transitions

$$f_{M\ell} = 10 f_{E\ell} \left(\frac{\hbar}{MCR}\right)^2, \qquad (28)$$

where R, M, D_0 and e are the nuclear radius, the mass of a proton, the spacing between low lying levels ~0.5 MeV and the charge of the electron, respectively. Assuming $R=1.25A^{1/3}$fm results in following transmission coefficients for gamma-radiation

$$T^{\sim}_{\gamma E1} = 2.71\cdot10^{-6}A^{2/3} E_\gamma^3 ,$$

$$T^{\sim}_{\gamma M1} = 7.80\cdot10^{-7} E_\gamma^3 . \qquad (29)$$

$$T^{\sim}_{\gamma E2} = 3.54\cdot10^{-12}A^{4/3} E_\gamma^5 . \quad E_\gamma \text{ in MeV.}$$

It is known that the single-particle model overestimates the transition strengths in comparison with experimental data even by three orders of magnitude, therefore eqs.(29) can be scaled by multiplicative factors CE1, CM1 and CE2, respectively, in order to bring the theoretical estimates into agreement with experimental radiative strenths. Comparison with results of average neutron resonance capture experiments [21] yields CE1=0.01, CM1=0.1 and CE2=0.1 for continuum transitions. For

transitions between low lying states the values CE1=0.01, CM1=0.1 and CE2=30 were obtained from spectroscopic studies.

The main contribution to the electric dipol transitions comes however from the decay of the giant dipole resonance (GDR) states. The strength of the GDR can be evaluated from the photoabsorption cross section [22]

$$\sigma_{\gamma E1} = 3\pi^2\hbar^2c^2 f_{E1} E_\gamma \qquad (30)$$

Assuming the Lorentzian shape for the GDR ,

$$\sigma_{\gamma E1} = \sum_{i=1}^{2} \frac{\sigma_i (\Gamma_i \Gamma_\gamma)^2}{(E_\gamma^2 - E_i^2)^2 + (\Gamma_i E_\gamma)^2} \ , \qquad (31)$$

and substituting (31) into (30) and the resulting strength function into (26) one obtains

$$T_{\gamma E1}^{GDR} = 5.46 \cdot 10^{-7} \sum_{i=1}^{2} \frac{\sigma_i \Gamma_i^2 E_\gamma^4}{(E_\gamma^2 - E_i^2)^2 + \Gamma_i^2 E_\gamma^2} \ , \qquad (32)$$

where σ_i (in mb), Γ_i and E_i are the peak cross section, the width and the energy of the splitted giant dipole resonance. The code allows a superposition of the GDR and the single-particle contributions

$$T_{\gamma E1} = (1-TE)\, T_{\gamma E1}^{W} + TE \cdot T_{\gamma E1}^{GDR} \ , \quad 0 \leq TE \leq 1 . \qquad 33$$

In case when the parameters of the GDR for a particular nucleus are lacking a single humped resonance of Lorentzian shape with global parameters is assumed: $\sigma_1 = 3\,\pi Z(A-Z)/A \cdot \Gamma_1$, $\Gamma_1 = 0.2 E_1$, $E_1 = 47.9\ A^{-0.2}$ [23]. Single humped M1 and E2 giant resonances can also be included into the calculation.

For radiative channels the summations in eqs. (7) to (7c) over the particle angular momentum j_x are properly replaced by sums over the final states spins $|I-l| \leq I_{b=\gamma} \leq |I+l|$ and the transition multipolarities l.

2.2 Pre-equilibrium emission

2.2.1 The geometry dependent hybrid model

Early comparisons between experimental results, exciton model calculations and intra-nuclear cascade calculations indicated that the exciton model gave too few pre-equilibrium particles and that these were too soft in spectral distribution. The comparison indicated that the exciton model deficiency resulted from a failure to properly describe the enhanced emission from nuclear surface. The first order correction to this deficiency was provided by the geometry dependent hybrid model [23](GDH), which assumes that the reaction proceeds in spherical shell-shaped regions of thickness $\lambda\alpha$ and radius determined by the projectile impact parameter. In this way the diffuse surface properties are sampled by the higher impact parameters.

The differential emission spectrum is given in the GDH model as

$$\frac{d\sigma(\varepsilon)^{GDH}}{d\varepsilon} = \pi\lambda_a^2 \sum_{\ell=0}^{\infty} (2\ell+1) T_\ell^a P_x^\ell(\varepsilon). \qquad (34)$$

The usual assumption that the composite system develops towards equilibrium via a sequence of states of icreasing complexity classified with the number of excited particles p and holes h, both referred as the excitons n=p+h, underlies the physical picture of the emission process. The initial state with n_0 excitons is formed as a result of interaction of the incoming particle with one of the target nucleons. The chain of the two-body interactions ends at the average exciton number characterising the equilibrium state $\bar{n}=\sqrt{2g\bar{E}}$. At each stage of the equilibration process the emission probability of neutrons x=ν or protons x=π with energy ε to $\varepsilon+d\varepsilon$ is calculated

$$P_x^\ell(\varepsilon)d\varepsilon = \sum_{\substack{n=n_0 \\ \Delta n=2}}^{\bar{n}} P_x^\ell(n,\varepsilon)d\varepsilon = \sum_{\substack{n=n_0 \\ \Delta n=2}}^{\bar{n}} p_x^n \left[\frac{\omega_{p,h}(U_x,\varepsilon) g_x}{\omega_{p,h}(E)} d\varepsilon\right] \left[\frac{\lambda_c(\varepsilon)}{\lambda_c(\varepsilon)+\lambda_+(\varepsilon)}\right] D_n. \qquad (35)$$

Here p_x^n is the fraction of the n excitons that are nucleons of type x, $\omega_n(U_x,\varepsilon)$ is the density of n exciton states, such that the nucleon if emitted, would have channel energy ε and leave the residual nucleus at excitation energy $U=E-B_x-\varepsilon$, where B_x stands for the binding energy of particle x, $\omega_n(E)$ is the Ericson's density of states [24], involving n excitons, g_x is the single-particle state density for nucleons x, $\lambda_c(\varepsilon)$ is the emission rate into the continuum, of a particle of channel energy ε, $\lambda_+(\varepsilon)$ is the intranuclear transition rate. The so-called depletion factor D_n represents the population surviving the particle emission from previous stages. The subscript l is introduced in the geometry dependent model to mark that all magnitudes entering the square brackets, but p_x^n depend on the entrance channel orbital angular momentum.

The fraction of the initial population, which has survived to a n-exciton configuration may be written

$$D_n = \prod_{n'=n_0+2}^{n} \left\{ 1 - \sum_x \int_0^{E-B_x} P_x^\ell(n'-2,\varepsilon)d\varepsilon \right\}. \qquad (36)$$

The GDH model employs the Fermi density distribution function

$$d(R) = d_s \left[\exp(R-C)/0.55\,fm + 1\right]^{-1}, \qquad (37)$$

with a charge radius $c=1.07\ A^{1/3}$fm and d_s taken from electron scattering results [25], for evaluating either the maximum or an average density along the projectile trajectory in the nucleus

$$\langle d \rangle = \int_0^{R_s} d(R)dR/R_s \quad , \text{ where } R_s=C+5\ 0.55\ \text{fm}. \qquad (38)$$

Formulae (37) and (38) are used to define the geometry dependent nuclear density and Fermi energy E_F according to the impact

parameter $R_l = \lambda_a(l+1/2)$ for each incoming partial wave.

$$\langle d(R_\ell)\rangle = \int_{R_\ell}^{R_s} d(R)\,dR/(R_s - R_\ell)\,, \tag{39}$$

$$E_F(R_\ell) = 40\left[\frac{\langle d(R_\ell)\rangle}{\langle d\rangle}\right]^{2/3}. \tag{40}$$

The Fermi energy has been taken 40 MeV for saturation density and was predicted, by the Fermi gas model, to vary as the average density to the two-third power. The value of $E_F(R_l)$ at each l is used for determining the single-particle level density

$$g(R_\ell) = 2g_x(R_\ell) = \frac{A}{14}\left[\frac{40}{E_F(R_\ell)}\right] = \frac{A}{14}\left[\frac{\langle d\rangle}{\langle d(R_\ell)\rangle}\right]^{2/3}. \tag{41}$$

Now all the terms entering the square brackets in formula (35) can be formulated. The second bracket contains the probability of particle emission. The emission rate into the continuum is expressed via the inverse reaction cross section

$$\lambda_c^\ell(\varepsilon) = \frac{(2s+1)}{\pi^2\hbar^3 g_x(R_\ell)}\, m\varepsilon\sigma_{inv}\,, \tag{42}$$

and the intranuclear transition rate is related to the mean free path (MFP) of the particle having velocity v, $\lambda_+(\varepsilon) = v/MFP$. The MFP can be evaluated either fromthe imaginary optical potential W [23],

$$MFP = \frac{\hbar}{W}\sqrt{\frac{(\varepsilon+V)}{2m}}\,, \tag{43}$$

or from the average nucleon scattering cross section $\bar{\sigma}^{NN}$ in nuclear matter of density d

$$MFP = [d\,\bar{\sigma}^{NN}(\varepsilon+V)]^{-1}. \tag{43a}$$

In the former case averaging along the trajectory of the particle results in

$$\langle W(R_\ell)\rangle = \int_{R_\ell}^{R_s} W(R)\,dR/(R_s - R_\ell), \text{ where } R_s = r_w A^{1/3} + 5a_w, \tag{43b}$$

r_w and a_w being the radius and the diffusivity of the imaginary optical potential, and

$$\lambda_+^\ell(\varepsilon) = \frac{\langle W(R_\ell)\rangle}{\hbar}\,. \tag{43c}$$

In the latter case one obtains

$$\lambda_+^\ell(\varepsilon) = \bar{\sigma}^{NN}(\varepsilon+V)\langle d(R_\ell)\rangle\sqrt{2(\varepsilon+V)/m}. \tag{43d}$$

The first of the brackets in formula (35) defines the fraction of the n=p+h exciton configurations having one of the p-particles in the continuum, at channel energy ε to $\varepsilon + d\varepsilon$. The

l-dependent state densities entering this probability will be discussed in the following. The p_x^n parameter determines the number of nucleons of given kind x in the n-exciton hierarchy. For the initial configuration with n_0 equal 3 this is

$$p_n^3 = \frac{2(3Z+2N)}{(6Z+2N)} \quad \text{and} \quad p_p^3 = 2 - p_n^3 \quad \text{for neutron projectile,}$$
$$p_p^3 = \frac{2(3N+2Z)}{(2Z+6N)} \quad \text{and} \quad p_n^3 = 2 - p_p^3 \quad \text{for proton projectile.} \tag{44}$$

Formulae (44) were obtained by assuming the free scattering cross section for unlike nucleons σ_{np} to be three times the cross section for like nucleons $\sigma_{nn} = \sigma_{pp}$ and by weighing the resulting configuration by the numbers of neutrons N and protons Z in the target [26].

By exploiting the naive dependence of the terms entering the emission probability expression (35), on the orbital angular momentum, in the entrance channel, one can now develop a cross section formula for the population of a final level with spin I_x and parity π_x, in the final nucleus after emission. Starting from the expression (34) and observing the conservation of the angular momentum throughout the formation and decay of the composite system one arrives at

$$\frac{d\sigma(U_x, I_x, \pi_x)}{dU_x}^{GDH} = \pi\lambda_a^2 \sum_{I^\pi=0}^{\infty} \sum_{S=|s_x-s_a|}^{s_x+s_a} \sum_{l=|I-S|}^{I+S} q_I T_l^a \sum_{\substack{n=n_0 \\ \Delta n=2}}^{\bar{n}} P_x^l(n,\mathcal{E}) \times$$
$$\times \left[\sum_{j_x=|I-I_x|}^{I+I_x} T_l^{j_x} \rho_{n-1}(U_x, I_x, \pi_x) \Big/ \sum_{I^{\pi'}=0}^{\infty} \sum_{j_x'=|I-I_x'|}^{I+I_x'} T_l^{j_x'} \rho_{n-1}(U_x, I_x', \pi_x') \right]. \tag{45}$$

Here, as in eqs. (7) and (7b), the parity selection rules are imposed implicitely as indicated by the subscript π. The coupling schemes for the angular momenta are the same as in eqs. (3) and (4). It should be emphasized that unlike in eqs. (7) and (7b) the spectral distributions of emitted nucleons, i.e. also the number of nucleons emitted with channel energy $\mathcal{E}$ to $\mathcal{E}+d\mathcal{E}$, is determined a priori by formula (34) and the term in square brackets in (45) defines only the spin distribution of levels in the residual nucleus, which are populated in the corresponding excitation energy interval U_x to U_x+dU_x.

The geometrical considerations based on the impact parameter imply the use of the l dependent transmission coefficients for calculation of the composite nucleus formation cross section in (45). Hence it is convenient to resort to the relation

$$T_l^a = \frac{l+1}{2l+1} T_l^{j_a=l+s_a} + \frac{l}{2l+1} T_l^{j_a=l-s_a} \tag{46}$$

2.2.2 Exciton-state densities in the GDH model

It has been concluded [4], that only for the initial configuration, $n_o = 3$, must the surface diffuseness be taken into account, in the densities of states $\omega_{p,h}$, because only then can an exciton acquire enough energy to sense the bottom of the potential well. This led to the combinatorial formulae

$$\omega_{2,1}(U,E) = \omega_{1,1}(U) = g E_F(R_\ell) \text{ and } \omega_{2,1}(E) = \frac{1}{4} g^2 E_F(R_\ell)[2E - E_F(R_\ell)], \quad (47)$$

for both U and $E > E_F(R_1)$. Originally the GDH model was formulated in terms of exciton energy partition functions, which however are equivalent to the densities of exciton states.

The state densities $\omega_{p,h}$ for configurations involving higher exciton numbers are calculated from the Ericson formula [24].

The particle-hole level densities $\rho_{n-1}(U_x, I_x, \pi_x) = \frac{1}{2}\rho_{n-1}(U_x, I_x)$ appearing in the square brackets of (45), are assumed to factorize into the energy dependent state density and the spin distribution part

$$\rho_{p,h}(U,I) = \omega_{p,h}(U) R_n(I) = \omega_{p,h}(U) \frac{2I+1}{2\sqrt{2\pi}\sigma_n^3} \exp\left[-\frac{(I+1/2)^2}{2\sigma_n^2}\right]. \quad (48)$$

The spin cut-off parameter σ_n was derived from combinatorial shell model calculations by Reffo and Herman [27] in a form: $(\sigma_n)^2 = 0.24^{2/3} n$. Similar calculation provides the energy of the yrast state as a function of its spin: $U_{yrast} = 75I^2/A^{4/3}(n-1/2)$ [MeV]. This relation allows to exclude the no-state region from the calculations. In practical computations n has been kept constant, equal to $(n_o - 1)$, which reflect the fact that the level densities are evaluated in the residual nuclei after emission of the first chance nucleon.

2.2.3 The multi-step compound emission

The quantum-mechanical statistical theory for PE emission was formulated by Feshbach, Kerman and Koonin [28] (FKK). These authors introduced two parallel PE reaction types. The first, referred to as multi-step compound (MSC) reaction, describes the flow of flux through a series of doorway states of increasing complexity, each of them containing only bound nucleons. The MSC mechanism gives rise to symmetric angular distributions of reaction products. The other, involving doorway states containing at least one particle in the continuum of states, which retains the memory of the incident channel, thus leading to forward peaked angular distributions, is called the multi-step direct reaction (MSD). The MSC formalism is incorporated into the EMPIRE code as an option for PE calculation.

The angle-integrated cross section formula derived in the framework of the FKK theory is similar to the ones known from the semiclassical models. The probability of formation of the composite system is given by the strength function for the formation of the first doorway state: $2\pi\lambda_a^2(2\pi\Gamma_1/D_1)$. The probabi-

lity of reaching the N^{th}-stage doorway state (equivalent to the depletion factor of eq. (35)) is,

$$P_N = \frac{\Gamma_{1,2}}{\Gamma_1} \cdot \frac{\Gamma_{2,3}}{\Gamma_2} \cdots \cdot \frac{\Gamma_{N-1,N}}{\Gamma_{N-1}} = \prod_{k=1}^{N-1} \frac{\Gamma_{k,k+1}}{\Gamma_k} \quad , \tag{49}$$

and the probability of emission from the N^{th}-stage is $\Gamma_e^N = \Gamma_N^\uparrow / \Gamma_N$, with $\Gamma_N^\uparrow$ being the emission width. Bearing in mind that $\Gamma_{N,N+1} = \Gamma_N^\downarrow$ is the spreading width and $\Gamma_N = \Gamma_N^\downarrow + \Gamma_N^\uparrow$, the product of the three probabilities can be rewritten in the following way

$$\frac{d\sigma^{MSC}}{dU} = \pi \lambda_a^2 \frac{2\pi \Gamma_1^\uparrow}{D_1} \sum_{N=2}^{\tau-1} \left(\prod_{k=1}^{N-1} \frac{\Gamma_k^\downarrow}{\Gamma_k} \right) \sum_{\nu=N-1}^{N+1} \frac{\Gamma_N^\uparrow}{\Gamma_N} \quad . \tag{50}$$

The fully equilibrated CN τ-stage is excluded from the first sum and the second sum reflects the fact that the emission from the N^{th}-stage bound state (embeded in the continuum) occurs indirectly via the continuum states involved in the MSD process. These continuum states can be reached in three different ways, $\Delta N = \pm 1, 0$ called exit modes. The summation over ν is just a summation over the possible exit modes.

In order to compute the cross section for population of a final state with energy U_b, spin I_b and parity π_b, b being the emitted particle, one has to include the angular momentum consideration into (50)

$$\frac{d\sigma(U_b, I_b, \pi_b)}{dU_b}^{MSC} = \pi \lambda_a^2 \sum_{I=0}^{\infty} g_I \frac{2\pi \Gamma_{1I}^\uparrow}{D_{1I}} \sum_{N=1}^{\tau-1} P_x^N \left(\prod_{k=1}^{N-1} \frac{\Gamma_{kI}^\downarrow}{\Gamma_{kI}} \right) \sum_{\nu=N-1}^{N+1} \left[\sum_{j_b=|I-I_b|}^{I+I_b} \left\langle \Gamma_{NI}^{j_b I_b \nu}(U_b) \varrho_\nu(U_b, I_b, \pi_b) \right\rangle / \Gamma_{NI} \right], \tag{51}$$

$$\text{with } \Gamma_{NI} = \Gamma_{NI}^\downarrow + \sum_\lambda P_\lambda^N \sum_{\nu=N-1}^{N+1} \sum_{I_b=0}^{\infty} \int_0^{E-B_\lambda} dU_\lambda \sum_{j_\lambda=|I-I_\lambda|}^{I+I_\lambda} \left\langle \Gamma_{NI}^{j_\lambda I_\lambda \nu}(U_\lambda) \varrho_\nu(U_\lambda, I_\lambda, \pi_\lambda) \right\rangle . \tag{52}$$

Formation of the initial doorway configuration from the entrance channel is approximated by the optical model strength function and, in the absence of microscopic evaluation, related to the partial wave transmission coefficients

$$2\pi \frac{\Gamma_{1I}^\uparrow}{D_{1I}} = R \left(\sum_{j_a=|I-s_T|}^{I+s_T} T_l^{j_a} \right) . \tag{53}$$

The reduction factor R takes into account the loss of flux due to direct and MSD processes. While no theoretical estimates of R are available it is evaluated from experimental data as a ratio of the symmetric portions of the angular distributions of

all reaction products to the reaction cross section [29]. For a different approach see ref. [30].

The term p_x^N is the same as (44), $p_x^N = q_x^N/(c_\nu^N + c_\pi^N)$, with c_x^N being the number of nucleons of given kind excited above the Fermi level. Here q_x^N is calculated from a recursive formula

$$q_\nu^{N+1} = p_\nu^N \frac{\sigma_{nn}}{\sigma_{nn}+\sigma_{np}} + p_\pi^N \frac{\sigma_{np}}{\sigma_{nn}+\sigma_{np}} + q_\nu^N \quad . \tag{54}$$

In case of incident neutrons the initial conditions are $c_\pi^0 = 0$ and $c_\nu^0 = 1$ and conversely for incident protons.

2.2.4 The particle-hole level densities and the transition widths in MSC reactions

The level densities appearing in eqs. (51) and (52) are particle-hole densities, which factorize with respect to the excitation energy U and level spin I as given by (48). However the state density $\omega_{p,h}$ now used has to contain only configurations having all particles bound. Such state densities have been derived algebraically with neglect of the Pauli exclusion principle and the finite well depth effect [31] and later with account for these effects [32]. The former are used in the code EMPIRE.

They have been obtained from a general formula for p-particles above the Fermi energy and h-holes below it, with total excitation energy E,

$$\omega_{p,h}(E) = \frac{p'!\,h'!\,(p-p')!\,(h-h')!}{p!\,h!} \int_0^E \omega_{p',h'}(\varepsilon)\,\omega_{p-p',h-h'}(E-\varepsilon)\,d\varepsilon \quad , \tag{55}$$

with $p' \leq p$, $h' \leq h$, $\omega_{10}(E) = g(E_F + E)$, $\omega_{01}(E) = g(E_F - E)$ and g(E) being the single-particle state density.

Equation (55) yields the well known Ericson formula for the equidistant spacings $g(\varepsilon) = g$ of the single-particle levels. The requirement of having all particles bound, imposed by MSC, can be formulated as $\omega_{10}(\varepsilon) = g$ or 0 for $\varepsilon \leq B$ or $\varepsilon > B$, respectively. The state densities calculated with the above restriction by Stankiewicz et al. [31] are labeled by the binding energy B,

$$\omega_{p,h}^B(E) = \frac{g^{p+h}}{p!\,h!} \sum_{i=0}^{I} \binom{p}{i} (-1)^i \frac{(E - iB)^{p+h-1}}{(p+h-1)!} \quad , \text{ for } IB < E \leq (I+1)B\,;\ I = 0,1,\cdots(p-1)$$

$$\omega_{p,h}^B(E) = \frac{g^{p+h}}{p!\,h!} \left\{ \sum_{i=0}^{p-1} \binom{p}{i} (-1)^i \frac{(E - iB)^{p+h-1}}{(p+h-2)!} + \right. \tag{56}$$

$$\left. - \sum_{i=0}^{p-1} \sum_{m=0}^{p-1} \binom{p}{i} (-1)^i \frac{(E - pB)^{h+m}\,[(p-i)B]^{p-m-1}}{(h+m)!\,(p-m-1)!} \right\}, \text{ for } E > pB \text{ and } p \leq h,$$

$$\omega^{B}_{p,h}(E) = \frac{g^{p+h}}{p!\,h!}\sum_{i=0}^{p-1}\sum_{m=0}^{h-1}\binom{p}{i}(-1)^{i}\frac{[(p-1)B]^{p+m}}{(p+m)!\,(h-1-m)!}(E-pB)^{h-1-m}, \quad \text{for } E>pB \text{ and } p\geq h. \tag{56}$$

The assumed energy-angular momentum factorization of the particle-hole level density (48) implies a similar factorization of all widths involved in the MSC process. The emission width then reads

$$\langle \Gamma^{j_b I_b \nu}_{NI}(U)\,\varrho_\nu(U_b,I_b)\rangle = Y^{\nu}_{N}(U_b)\,X^{j_b I_b \nu}_{NI}(U_b)\,. \tag{57}$$

The MSC theory uses the subscript N for marking the stage in the interaction chain, from which the emission takes place. The ambiguity between N and the number of excitons n, which marks the particle-hole level density, can be removed by adopting the exciton representation for the partition of the doorway states. In this case $n=p+h=2N+1$. This relationship will however not be used, since as we will see below the densities of states accessible in the possible exit modes depend only on the number of excitons, which immediately participate in the interaction. The remaining core excitons or observers do not count.

The Y functions in eq. (57) contain all the U dependence originating in the final state level density, while the functions X contain the angular momentum structure embodied in the residual interaction force of δ-tyre and the assumed spin distribution of the single-particle levels $gR_1(I)$ [28], with $R_1(I)$ taken from (48) at $n=1$.

We now evaluate the $Y^{\nu}_{N}(U)$ function, which is the density of states accessible in the possible exit modes $\nu = N\pm1,\ N$.

For $\nu = N$, particle emission, without change in the number of particles and holes, can take place if a particle collides with another particle or with a hole, and is scattered into the continuum. The particle-particle collision can take place in $(1/2)\,p(p-1)$ ways, so that

$$_{pp}Y^{N}_{N} = \frac{1}{2}p(p-1)g\,P^{p-2,h}_{ph}(U)\,, \tag{58}$$

where $P^{p-2,h}_{ph}(U)$, the probability that after separation of the interacting particle pair the remaining nucleons have an excitation energy not greater than U, correspondingly to the energy of the emitted particle from 0 to E-B-U, can be expressed as the ratio of the density of states with (p-2) particles and h holes and with excitation energy less or equal U, to the density for p particles and h holes at excitation E

$$_{pp}Y^{N}_{N} = \frac{1}{2}p(p-1)g\,\frac{1}{\omega^{B}_{ph}(E)}\,\frac{2!(p-2)!}{p!}\int_{0}^{U}\omega^{B}_{20}(E-z)\,\omega^{B}_{p-2,h}(z)\,dz\,. \tag{59}$$

Similarly the particle-hole collision can take place in ph ways so that

$$ {}_{ph}Y_N^N = phg P_{ph}^{p-1,h-1}(U) = phg \frac{1}{\omega_{ph}^B(E)} \frac{(h-1)!(p-1)!}{p!h!} \int_0^U \omega_{1,1}^B(E-z)\omega_{p-1,h-1}^B(z)dz . \qquad (60) $$

The sum of both ${}_{pp}Y_N^N$ and ${}_{ph}Y_N^N$ after conducting the integrations provides

$$ Y_N^N = Bg^2 h \frac{\omega_{p-1,h}^B(U)}{\omega_{p,h}^B(E)} + \alpha \frac{1}{2}(h+1)(h+2)\frac{g}{\omega_{p,h}^B(E)}\left[\frac{U-E+2B}{h+2} g\omega_{p-2,h+1}^B(U) + \right. \qquad (61) $$

$$ \left. + \beta\omega_{p-2,h+2}^B(E-2B) - \omega_{p-2,h+2}^B(U)\right] , $$

with $\alpha = 1$ for $E \leq 2B+U$, $\beta = 1$ for $E > 2B$ and both equal 0 elsewhere.

For $Y = N+1$, a particle undergoes scattering with the simultaneous creation of a particle-hole pair or a hole scatters with creation of a particle-hole pair, the particle of which is emitted. The first case does not contribute to emission because a particle occupying the bound orbital can only loose energy in such interaction. It contributes however to the damping width with no particle emission. The corresponding Y_N^{N+1} functions are products of the number of ways of choosing the interacting particle or hole from the p+h excitons, the density of states accessible to the created particle-hole pair, and the probability that the noninteracting, core excitons have exactly the energy U-t, where t is the particle-hole pair energy. The latter probability is

$$ P_{ph}^{\prime p-1,h}(U-t) = \frac{d}{dx} P_{ph}^{p-1,h}(x)\Big|_{x=U-t} = \frac{1}{p\omega_{ph}^B(E)} \omega_{10}^B(E-U+t)\omega_{p-1,h}^B(U-t). \qquad (62) $$

Integrating over the energy of the particle-hole pair t gives

$$ {}_pY_N^{N+1} = p\int_0^U dt\, \omega_{1,1}^B(t)\, P_{ph}^{\prime p-1,h}(U-t) , \qquad (63) $$

$$ {}_hY_N^{N+1} = h\int_0^U dt\, \omega_{02}(t)\, P_{ph}^{\prime p,h-1}(U-t) . \qquad (64) $$

The density of states available to the created particle-hole pair is $\omega_{1,1}^B(t) = g^2 \cdot \min(t,B)$ and for the pair of holes remaining

in the system $\omega_{02}(t)=\frac{1}{2}g(gt)$. Conducting the integration in (64) provides

$$Y_N^{N+1} = \frac{1}{2} gh(h+1) \frac{\omega^B_{p,h+1}(U)}{\omega^B_{ph}(E)} \tag{65}$$

After adding (63) and (64) and integrating within the limits E-B and E, which do not allow the interacting particles to escape one obtains the damping with,

$$Y_N^{N+1\downarrow} = g \frac{(h+1)(h+2)}{\omega^B_{ph}(E)} \Big\{ \frac{1}{2} h \omega^B_{p,h+2}(E) - \alpha \frac{1}{2} h \omega^B_{p,h+2}(E-B) + (h+3)\omega^B_{p-1,h+3}(E)$$

$$- \alpha \Big[(h+3)\omega^B_{p-1,h+3}(E-B) + \frac{g^2 B}{2(h+2)} \omega^B_{p-1,h+1}(E-B) + gB\omega^B_{p-1,h+2}(E-B) \Big] \Big\}, \tag{66}$$

with α equal 1 for $E > B$ and 0 for $E \leq B$.

In the $\nu = N-1$ case, a particle is emitted with simultaneous annihilation of a particle-hole pair. A similar consideration leads to

$$Y_N^{N-1} = \frac{1}{2} hp(p-1) \frac{d}{dx} P^{p-2,h-1}_{ph}(x) \Big|_{x=U} = \frac{\omega^B_{21}(E-U)\omega^B_{p-2,h-1}(U)}{\omega^B_{ph}(E)} . \tag{67}$$

The angular momentum structure of the X^{jbIb}_{NJ} function is obtained by evaluation of the transition matrix element. The contributing terms come from the initial and final wave functions, the interaction potential and the spin derendence of the level density. The matrix element for an antisymmetric two-particle wave function, of the delta interaction potential $V(\vec{r}_1, \vec{r}_2) = V_0(\frac{4}{3}\pi r_0^3)\delta(r_1 - r_2)$, has been derived by Stankiewicz and Marcinkowski [33].

$$\Delta_{if} = \alpha I^{n_4\lambda_4 n_3\lambda_3}_{n_1\lambda_1 n_2\lambda_2} \sqrt{(2S+1)(2Q+1)(2j_3+1)(2j_4+1)(2j_2+1)(2l+1)} \begin{Bmatrix} j_3 & l & Q \\ I & j_4 & s \end{Bmatrix} \begin{pmatrix} l & j_3 & Q \\ \frac{1}{2} & -\frac{1}{2} & 0 \end{pmatrix} \begin{pmatrix} j_2 & j_4 & Q \\ \frac{1}{2} & -\frac{1}{2} & 0 \end{pmatrix}, \tag{68}$$

for $\lambda_4 + \lambda_3 + Q$ and $\lambda_1 + \lambda_2 + Q$ even or 0 otherwise. Here α is the phase factor $(-1)^{j_4+S+Q+\lambda_4+j_2+\lambda_1+1}$ and the radial overlar integral reads.

$$I^{n_4\lambda_4 n_3\lambda_3}_{n_1\lambda_1 n_2\lambda_2} = \frac{V_0}{4\pi}\left(\frac{4}{3}\pi r_0^3\right) \int_0^\infty R^*_{n_1\lambda_1} R^*_{n_2\lambda_2} R_{n_3\lambda_3} R_{n_4\lambda_4} \frac{d\tau}{\tau^2} . \tag{69}$$

The indexing of the quantum numbers (main-n, orbital-λ and total angular momentum-j) of the interacting excitons is clarified in fig.3. For conveniency j_b=1 and I_b=s is used beneath.

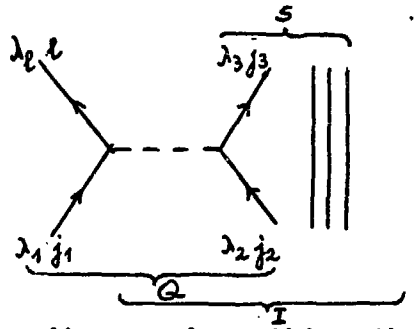

Fig. 3 The diagram describing the angular momentum coupling in particle-particle scattering relevant for the X_N^N function

In computing the $X_{NI}^{j_b I_b}$ functions only the square of the particle-particle matrix element is used, since particle-hole distinguishability was treated in counting for the Y functions. To find X the square of the matrix element has to be averaged over initial configurations, summed over final states and multiplied by 2π. Thus for $\nu = N$

$$X_{NI}^{\ell s N} = 2\pi \sum_{Q j_1 j_2 j_3 j_4} \frac{R_2(Q) R_{N-2}(j_4)}{R_N(I)} \frac{R_1(j_1) R_1(j_2)}{R_2(Q)} (2j_1+1)(2j_2+1)(2Q+1) \times$$
$$\sum_{j_3} R_1(j_3)(2j_3+1)(2\ell+1)(2s+1) \begin{Bmatrix} j_3 & \ell & Q \\ I & j_4 & s \end{Bmatrix}^2 \begin{pmatrix} \ell & j_3 & Q \\ \frac{1}{2} & -\frac{1}{2} & 0 \end{pmatrix}^2 \begin{pmatrix} j_1 & j_2 & Q \\ \frac{1}{2} & -\frac{1}{2} & 0 \end{pmatrix}^2 I_\ell^2 , \qquad (70)$$

or

$$X_{NI}^{\ell s N} = 2\pi \frac{(2\ell+1)(2s+1)}{R_N(I)} I_\ell^2(U) \sum_{Q j_3 j_4} (2Q+1) F(Q) R_1(j_3) R_{N-2}(j_4)(2j_3+1) \begin{pmatrix} \ell & j_3 & Q \\ \frac{1}{2} & -\frac{1}{2} & 0 \end{pmatrix}^2 \begin{Bmatrix} j_3 & \ell & Q \\ I & j_4 & s \end{Bmatrix}^2 \qquad (71)$$

with $F(Q) = \sum_{j_1 j_2} (2j_1+1)(2j_2+1) R_1(j_1) R_1(j_2) \begin{pmatrix} j_1 & j_2 & Q \\ \frac{1}{2} & -\frac{1}{2} & 0 \end{pmatrix}^2 .$

The first sum in eq.(70) with the weighting factors assuring proper angular momentum structure of the initial configuration stands for averaging over the initial states. Together with summation over final states j_3 it entails introducing an average radial integral $I_1(U)$ free of details of the wave functions (1 and U distinguish the continuum wave function only).

For $\nu = N \pm 1$ one obtains similarly

$$X_{NI}^{\ell s N+1} = 2\pi \frac{(2\ell+1)(2s+1)}{R_N(I)} I_\ell^2(U) \sum_{Q j_3 j_4} (2Q+1) R_1(Q)(2j_3+1) F(j_3) R_{N-1}(j_4) \begin{pmatrix} \ell & Q & j_3 \\ \frac{1}{2} & -\frac{1}{2} & 0 \end{pmatrix}^2 \begin{Bmatrix} j_3 & \ell & Q \\ I & j_4 & s \end{Bmatrix}^2, \quad (72)$$

with $F(j_3) = \sum_{j_1 j_2} (2j_1+1) R_1(j_1)(2j_2+1) R_1(j_2) \begin{pmatrix} j_1 & j_2 & j_3 \\ \frac{1}{2} & -\frac{1}{2} & 0 \end{pmatrix}^2$ and

$$X_{NI}^{\ell s N-1} = 2\pi \frac{R_{N-3}(s)}{R_N(I)} I_\ell^2(U) \sum_{Q j_3} (2Q+1) F(Q)(2j_3+1) R_1(j_3) \begin{pmatrix} \ell & j_3 & Q \\ \frac{1}{2} & -\frac{1}{2} & 0 \end{pmatrix}^2 \Delta(\ell s I), \quad (73)$$

with $\Delta(lsI)$ equal 1 for $|l-s| \leq I \leq l+s$ and 0 otherwise. Eventually

$$X_{NI}^{\downarrow} = 2\pi \frac{1}{R_N(I)} I_B^2 \sum_{Q j_4} R_1(Q) \tilde{F}(Q) R_{N-1}(j_4), \quad (74)$$

where $\tilde{F}(Q) = \sum_{\ell} \sum_{j_3} (2j_3+1) F(j_3)(2\ell+1) R_1(\ell) \begin{pmatrix} \ell & Q & j_3 \\ \frac{1}{2} & -\frac{1}{2} & 0 \end{pmatrix}^2$.

For diagrams representing the angular momentum coupling for the $\nu = N+1$ exit nodes the reader is referred to ref. [27]. The total width calculated according to eq.(52) contains a sum of the X-functions over I_b=s, this can be conveniently done by using the completeness relation for the 6-j and 3-j coefficients [28]. In the light of the approximations done it is possible to evaluate the scale of the overlap integrals assuming all the radial wave functions as constant inside the nuclear volume. this yields,

$$2\pi I_B^2 = 2\pi \frac{V_0^2}{A^2} \quad \text{and} \quad 2\pi I_{\ell_b}^2(U) = \frac{4}{3} \frac{V_0^2 r_0^3 k m T^{\ell_b}}{\hbar^2 A}. \quad (75)$$

used in the EMPIRE code.

3. Structure of the program

The code EMPIRE is organized as shown in fig. 4. At the very beginning the tables of j-dependent partial wave transmission coefficients are calculated with use of the SCAT [14] subroutine and level densities are calculated for all channels and the corresponding nuclei under consideration on the first chance emission stage of the reaction N=1. The continuum levels in each nucleus are discretized into energy bins of width ΔU, each of them containing $\rho(U,I,\pi)\Delta U$ levels placed in the centre of the bin. In the first stage the PE emission of protons and neutrons is allowed.

If the PE option is selected, HYBR=1 or HYBR > 1, spectra of emitted nucleons are calculated with the use of the HYBRID [4] or the MSC subroutines, respectively. The populations of levels both discrete and in the continuum are calculated from formulae (45) or (51) for the residual nuclei after neutron and proton emission. The populations of the continuum states are recorded on the local files ascribed to the two residual nuclei involved. The factor R^1 (see description of eq. (5)) are computed and stored to be used in normalization of the equilibrium calculation (see eq. (7)).

The population of levels, continuum and discrete, of the CN, resulting from the projectile capture, as well as those resulting from the decay of the CN into theassumed channels are calculated according to formula (7). The partial cross sections for the particle emission are labelled by the energy bin, the spin and the parity of the populated level and stored on local files. The PE nucleon cross sections labelled accordingly being added. The radiative transitions between and from the energy bins in the continuum, and optionally between the discrete levels are calculated in competition with the energetically allowed emission of particles, thus providing the populations of the continuum and discrete levels of the CN. These calculations result in the cross sections for gamma-ray production and population of discrete levels, e.g. isomeric states in the CN. In addition to the "full gamma cascade" mode, GST=0, described above three other options are available, which reduce the CPU time required. The first one stops the gamma-ray cascade at the particle binding energy level. Within this option the cross sections for particle emission are calculated but the gamma-ray spectra and level populations in the CN are deformed. The second option allows for primary radiative transitions from the capturing state of the CN only and greatly reduces the computation time. It provides approximate radiative capture cross sections and exact primary gamma-ray spectrum. The third possibility allows one to eliminate the gamma transitions from consideration. This option is suggested at the first stage of reaction involving multi-particle emission. The capture cross section is negligible in such cases.

If the width fluctuation effects, in the decay of the capturing states, are important, FLUC=0, the cross sections at the first stage are calculated according to the HRTW approach [9] (eq. (7b-c)). The iteration scheme (11)-(12) is continued until the accuracy of 0.1% is achived.

The final population of discrete levels in the CN preceded by the particle and gamma-ray spectra are printed at the end of the 1st stage of reaction.

In the case of a reaction involving multi-particle emission (E > 0, AD≠0 in card No 39) new tables of transmission coefficients and level densities are calculated repeatedly at each stage and all information pertaining the residual nucleus at the stage under consideration replaces in the memory the information concerning the preceding stage of the process. The appropriate local file is filled, sorted and summed up to give the population of the continuum and discrete levels of the nucleus of interest. Its decay is calculated in a way analogous to that described above. Such procedure is repeated until the list of subsequently emitted particles is exhausted.

3.1 Restrictions on the complexity of the computational problem

Particles considered in the program are neutrons, protons and alphas. In addition deuterons in the entrance channel and gammas in the exit channels are included. The PE emission does not allow for alpha particles.

The maximum energy and number of subsequently emitted particles are not restricted in the code but the energy discretization of the continuum is confined to 120 bins, which puts a limit on the accuracy of the integration procedure.

The maximum number of partial waves considered in the calculation is 30. Only E1, M1 and E2 gamma-transitions are allowed to contribute to the gamma cascade. Up to 50 discrete levels for each nucleus taken into account can be used. In the gamma-decay of these levels up to 11 transitions depopulating each level might be concerned.

The running time depends strongly on the composite nucleus excitation energy, the energy integration step, the number of involved channels, partial waves and reaction stages. A typical running time for a (n,2n) reaction, at an energy equal 14 MeV and for integration step equal 1 MeV, involving 14 partial waves and all allowed competitions, is about 10 min on a CYBER 73 computer.

4. Comparison of calculations with experimental data

In 1985 an international effort has been undertaken to compare statistical nuclear reaction models and codes that calculate reaction cross sections, emission spectra and angular distributions, with account for both the evaporation from the CN and the PE emission. These models are widely used in cross section evaluations for technological applications, in the projectile energy interval from 0.5 MeV to 30 MeV, which is also of particular interest for testing nuclear models because the reaction mechanism changes in this region. Usually the interaction appears predominantly compound just above the reaction threshold and changes with increasing energy to predominantly PE and direct. The codes, which use the Hauser-Feshbach theory and have contributed to the intercomparison exercise are

listed in table I.

Table I. Contributions to model and code comparison

Code name	Contribution/Laboratory	Reference
STAPRE	S. Wilbholak, B. Strohmaier M. Uhl/IRK+	[34]
SMASH	P.G. Young/LAS	[35]
HAUSER-Y	S.P. Garg, A. Sinha/TRM	[36]
PERRINI	H. Grurrelaar, H.A.J. Van der Kamp/ECN	[37]
TNG	C.Y. Fu/ORL	[38]
EMPIRE	M. Herman/IBJ	[9]

+/GIND' convention

These codes classified according to ref. [10] as class A codes are time consuming and require large computer memory. All but EMPIRE use for calculation of the PE emission the exciton model, which treats also the emission of alpha particles.

The overall results of the computations are quite consistent for the neutron scattering reactions (n,n') and (n,2n), though deviations exist between particular calculations and/or experiments at low and high energy ends of the neutron spectra, fig. 5. These deviations are related to the energy grid size, pairing energy shifts, geometry effects and effects due to excitation of individual excited levels. The GDH model seems to mask best the deficiency of not accounting, by all the models, for the collective excitations at low energies.

For the much smaller (n,p) and (n,α) reaction cross sections large deviations were established. In this case there is no significant difference between the results of the more sophisticated and time consuming codes and those using the Weisskopf-Ewing formula and some simple formulations of the exciton model.

The EMPIRE code is particularly suitable for complete data evaluations, like the one in fig. 6, for the neutron induced reactions on ^{62}Ni. Such complete analyses can be carried out or depending on whether the objective is to obtain a good fit to a choosen data set [39,40] see also figs. 7 and 8, or whether it is to describe a wide-range of data with the least number of parameters. The latter, global parameterization method, is often used in neutron data evaluation, though it usually fails in providing adequate details, like e.g. cross sections for sequences of target isotopes, fig. 9.

The application of the MSC model has been extended to the area, where one may expect this reaction mechanism to contribute significantly, namely to the (n,2n) reaction , which involves the soft part of the neutron emission spectrum and therefore should not be affected to greater extent by simpler processes, e.g. by the statistical MSD reactions. The early calculations

of the $^{93}Nb(n,2n)$, $^{93}Nb(n,\gamma)$ and $^{181}Ta(n,2n)$ reaction cross sections [29] were very encouraging, figs. 10 and 11. The more advanced calculations using formulae (56) to (75) or the overlap integrals with the wave functions generated in a harmonic oscillator potential [1] have shown that the results are not yet fully satisfactory, as shown in fig. 12. The MSC model in EMPIRE has the tendency to provide a PE spectrum of emitted nucleons, which is softer than that of the GDH model. It displays too few high energy nucleons and too many in the intermediate spectral energy region, providing simultaneously too high PE yield.

The main task in conducting any of such calculation is a consistent parameterization of (i) the optical model potentials, (ii) the level and state densities and (iii) the radiative strength functions. EMPIRE offers a wide choice of optical potentials, as described in sect. 2.1.4, and the level densities have been carefully parameterized in refs. [12,13]. The radiative strength function for the GDR are available, e.g. from ref. [41].

6. Conclusions

The code EMPIRE is apt to calculate a variety of cross sections for an evaporation sequence from a CN . The gamma-ray cascades are treated in great detail. The inclusion of the PE decay in the first step processes, for which the CN concept is not adequate enough, validate the calculations of particle emission spectra especially for heavier target nuclides. Nevertheless there remain cross sections of some practical importance, which can not be reliably evaluated with use of EMPIRE. Some of the constraints have been mentioned in the 1st section. Other like the excitation of low lying collective states is not included in the existing versions of the PE models and has to be calculated with use of direct reaction theories. The radiative capture of nucleons at higher incident energies is well described by the semidirect mechanism, involving the excitation of the GDR, which is also not contained in the formalism described. This influences the high energy part of the gamma-ray production cross sections at high incident energy. Still the code has proved well in describing the main body of the fast neutron induced reactions, low energy neutron and proton capture, as well as the accompanying gamma-ray production cross sections.

References

1. Marcinkowski A., Proc. Int. Conf. on Fast Neutron Phys., Dubrovnik, Yugoslavia, 1976, INDC YUG -010/G
2. Adamski L., Herman M. and Marcinkowski A., Final Report, IAEA Research Contract no 2741/RB, (1983)
3. Blann M. and Vonach H.K., Phys. Rev. C28 (1983) 1475
4. Blann M., Report COO-3494-14 1974 ; Phys. Rev. Lett. 28 (1972) 757
5. Feshbach H., Rev. Mod. Phys. 46 (1974) 1
6. Bonetti R., Colli Milazzo L., De Rosa A., Inglima G., Perillo E., Sandoli M. and Shabin P., Phys. Rev. C21 (1980) 816

7. Tepel J.W., Hofmann H.M. and Weidenmüller H.A., Phys. Lett. B49 (1974) 1

8. Hofmann H.M., Richert J., Tepel J.W. and Weidenmüller H.A., Ann. Phys. 90 (1975) 403

9. Herman M., Marcinkowski A. and Stankiewicz K., Comp. Phys. Comm. 33 (1984) 373

10. Gruppelaar H. and Nagel P., Report on Int. Nuclear Model and Code Comparison, NEANDC-204 U, NEA Data Bank, (1985)

11. Hofmann H.M., Mertelmeier T., Herman M. and Tepel J.W., Z. Phys. 297 (1980) 153

12. Cameron A.G.W. and Gilbert G., Can. J. Phys. 43 (1965) 1446

13. Reffo G., CNEN Report RT/FI (78) 11, Bologna (1978)

14. Smith W.R., Comp. Phys. Comm. 1 (1969) 106

15. Moldauer P.A., Nucl. Phys. 47 (1963) 65

16. Björklund F., Fernbach S. and Shermon M., Phys. Rev. 103 (1958) 1295

17. Becchetti F.D. and Greenlees G.W., Phys. Rev. 182 (1969) 1190

18. Wilmore D. and Hodgson P.E., Nucl. Phys. 55 (1964) 673

19. McFadden L. and Satchler G.R., Nucl. Phys. 84 (1966) 177

20. Blatt J.M. and Weisskopf V.F., Theoretical Nuclear Physics Wiley, New York, 1952

21. Bollinger L.M. and Thomas G.E., Phys. Rev. C2 (1970) 1951

22. Axel P., Phys. Rev. 126 (1962) 671

23. Blann M., Nucl. Phys. A213 (1973) 570

24. Ericson T., Adv. in Phys. 9 (1960) 425

25. Hofstadter R., Ann. Rev. Nucl. Sci. 7 (1957) 295

26. see ref. 3

27. Reffo G. and Herman M., Nuovo Cimento Lett. 34 (1982) 261

28. Feshbach H., Kerman A. and Koonin S., Ann. Phys. 125 (1980) 429

29. Herman M., Marcinkowski A. and Stankiewicz K., Nucl. Phys. A430 (1984) 69

30. Holler V., Kaminsky A., Langkau R., Seebel W., Trabandt M. and Bonetti R., Nucl. Phys. A442 (1985) 79

31. Stankiewicz K., Marcinkowski A. and Herman M., Nucl. Phys. A435 (1985) 79

32. Obložinsky P., Nucl. Phys. A453 (1986) 127

33. Stankiewicz K. and Marcinkowski A., unpublished

34. Strohmaier B. and Uhl M., in Nuclear Theory for Applications

IAEA-SMR 43, 313 (1980)

35. Young P.G. and Arthur E.D., Los Alamos Report LA-6947

36. Mann F.M., HEDL-TME-78-83 (1979)

37. Drupsteen H., unpublished

38. Fu C.Y., Brookhaven Report BNL-NCS-51245, Vol.2, 675 (1980)

39. Andersson P., Zorro R., Bergqvist I., Herman M. and Marcinkowski A., Nucl. Phys. A443 (1985) 404

40. Marcinkowski A., Stankiewicz K., Taruska U. and Herman M., Z. Phys. 323 (1986) 91

41. Fuller E.G., Gerstenberg H.M., Van der Molen H. and Dunn P.C., Photonuclear Reaction Data, National Bureau of Standards Report (1973)

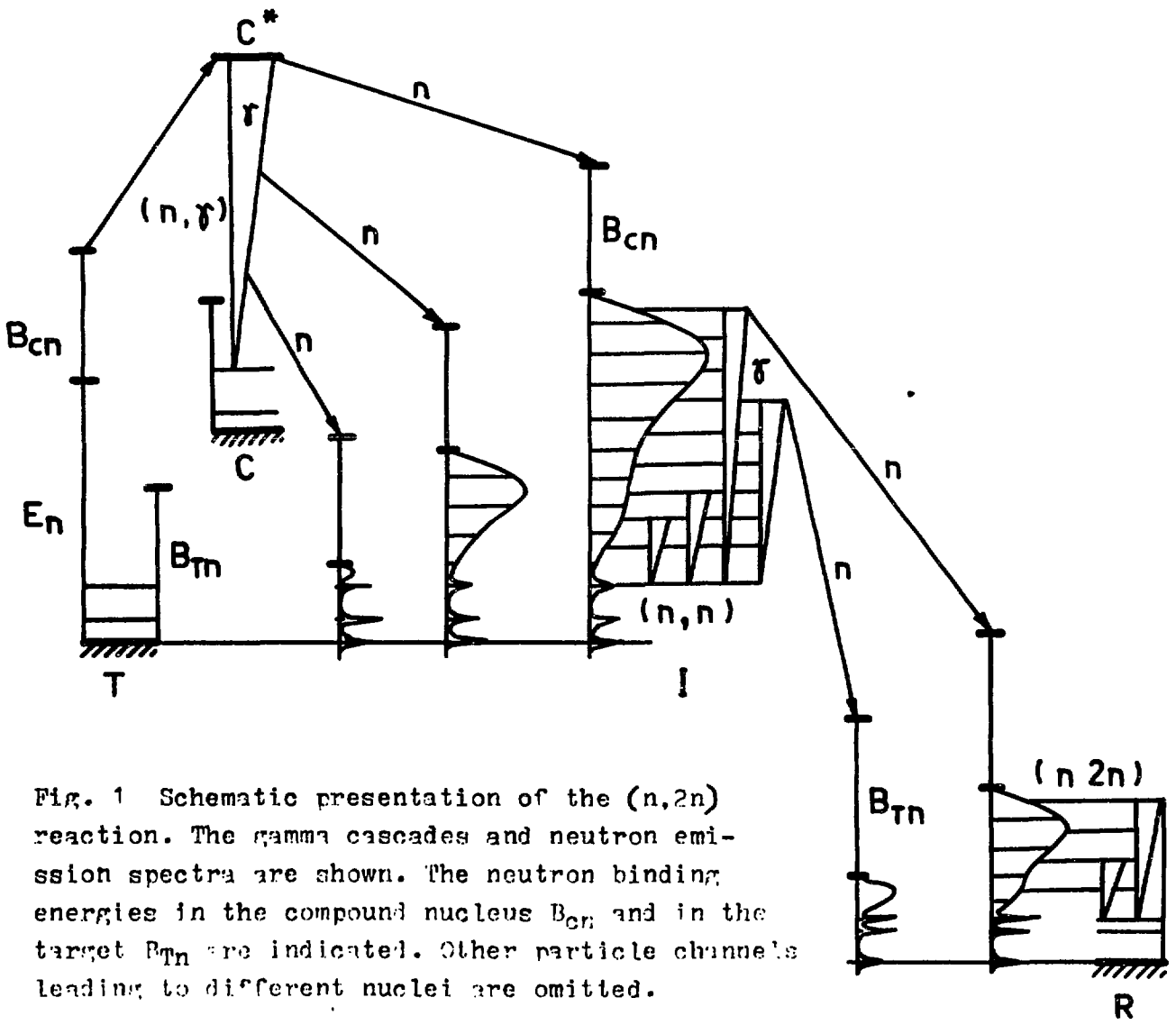

Fig. 1 Schematic presentation of the (n,2n) reaction. The gamma cascades and neutron emission spectra are shown. The neutron binding energies in the compound nucleus B_{cn} and in the target B_{Tn} are indicated. Other particle channels leading to different nuclei are omitted.

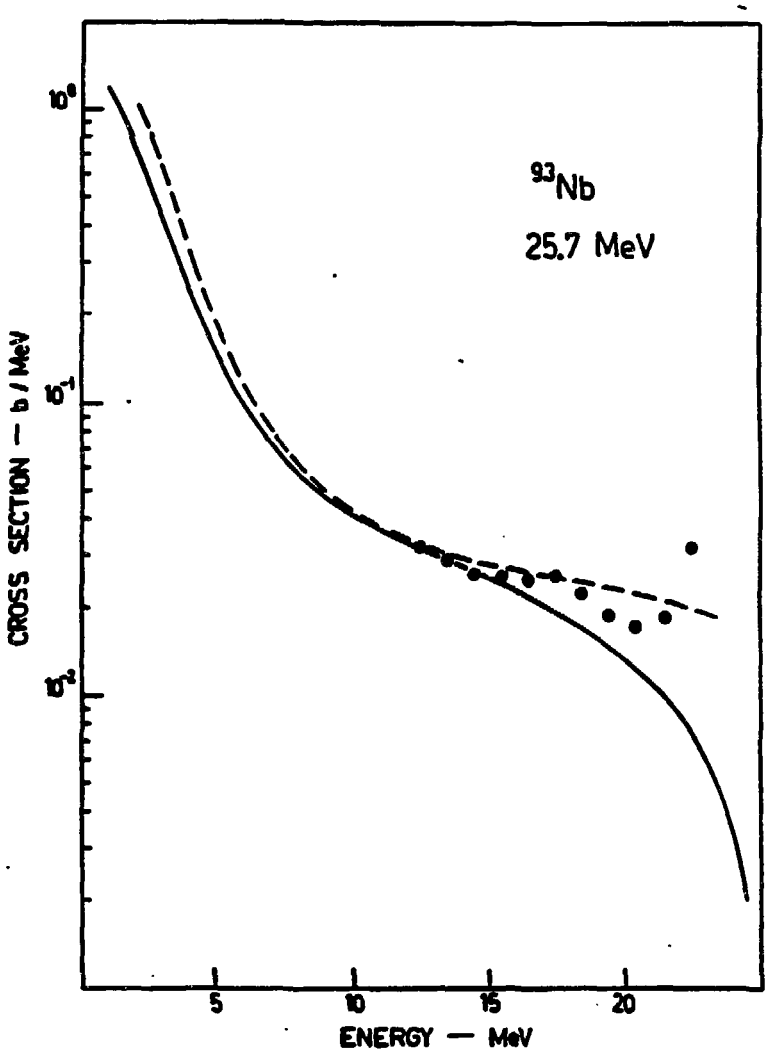

Fig. 2 Comparison between the calculated and the measured neutron spectra from the reaction ^{93}Nb + n at 25.7 MeV. The dashed line was obtained from EMPIRE and the solid one from GNASH.

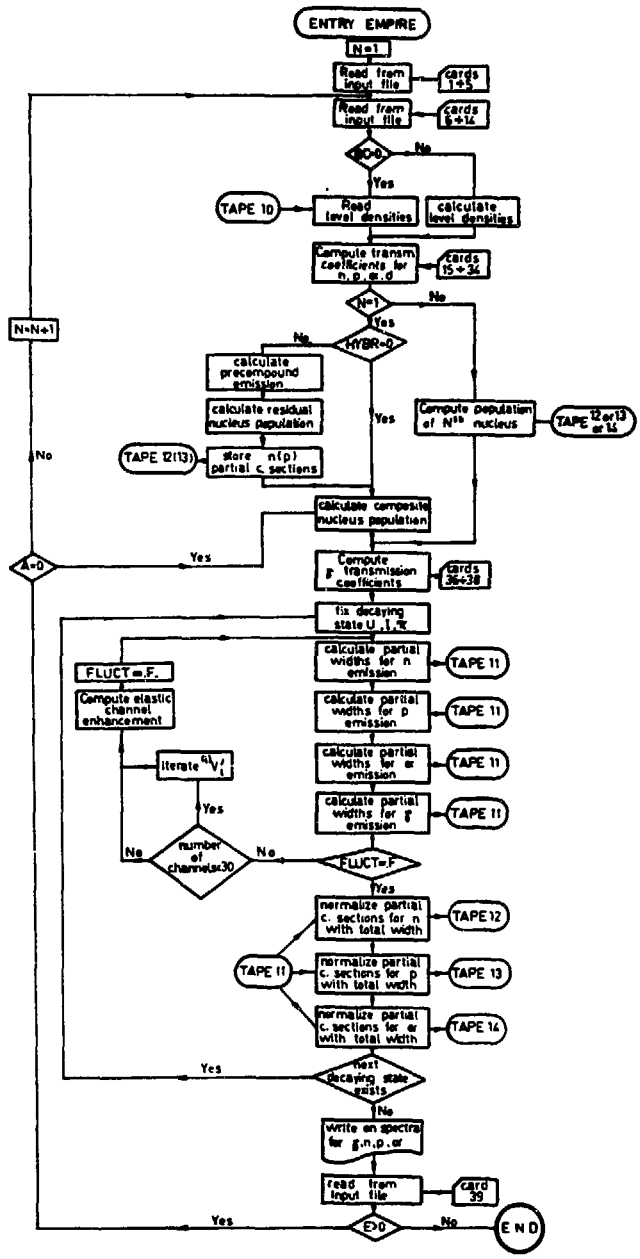

Fig. 4 The flow diagram of the EMPIRE code.

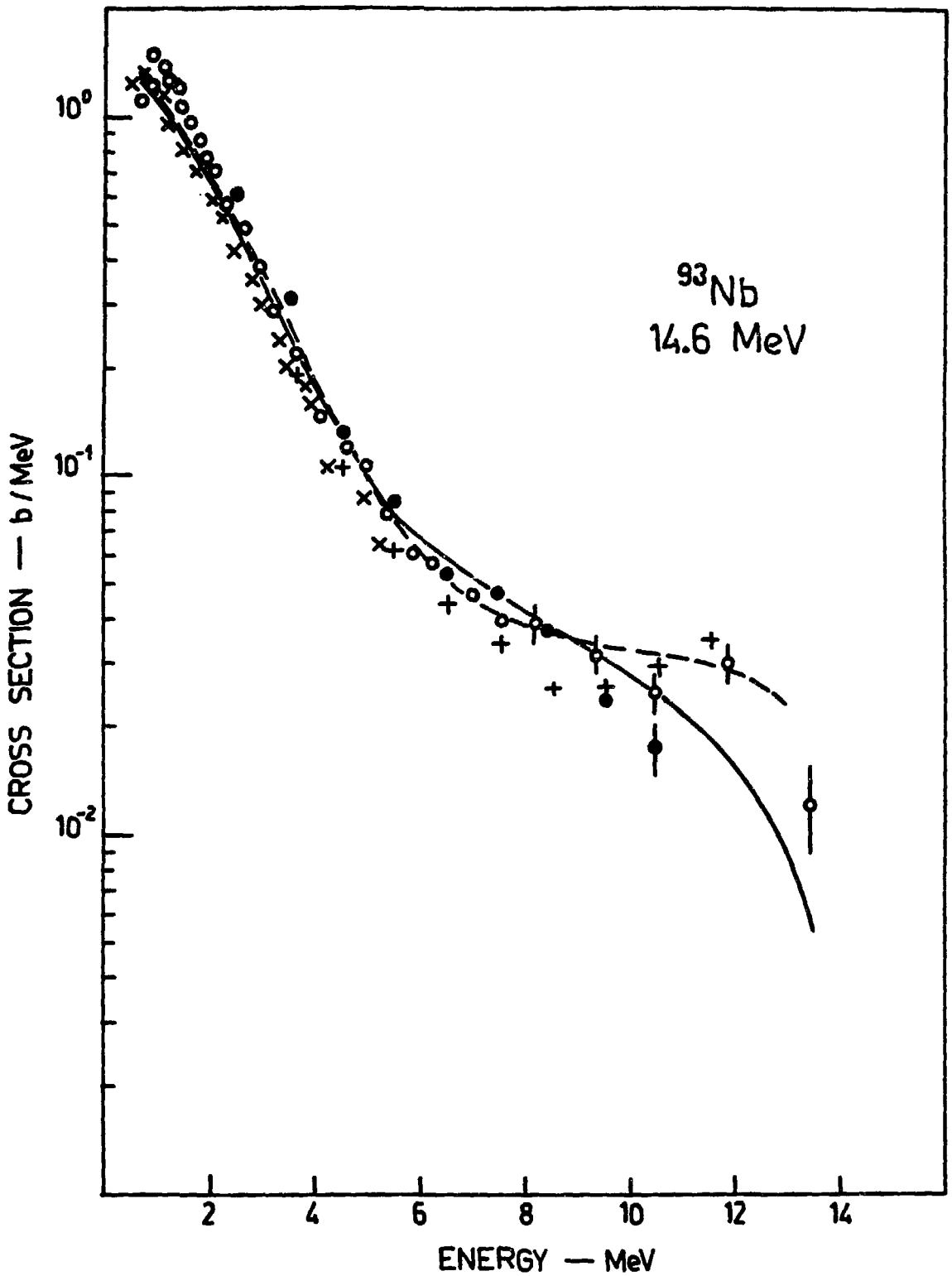

Fig. 5 Comparison of the total neutron emission spectra at 14.6 MeV, calculated with use of EMPIRE (dashed line) and SNASH (solid line), with experiments: closed circles - Technical University Dresden, crosses - Osaka University and open circles - Obninsk data.

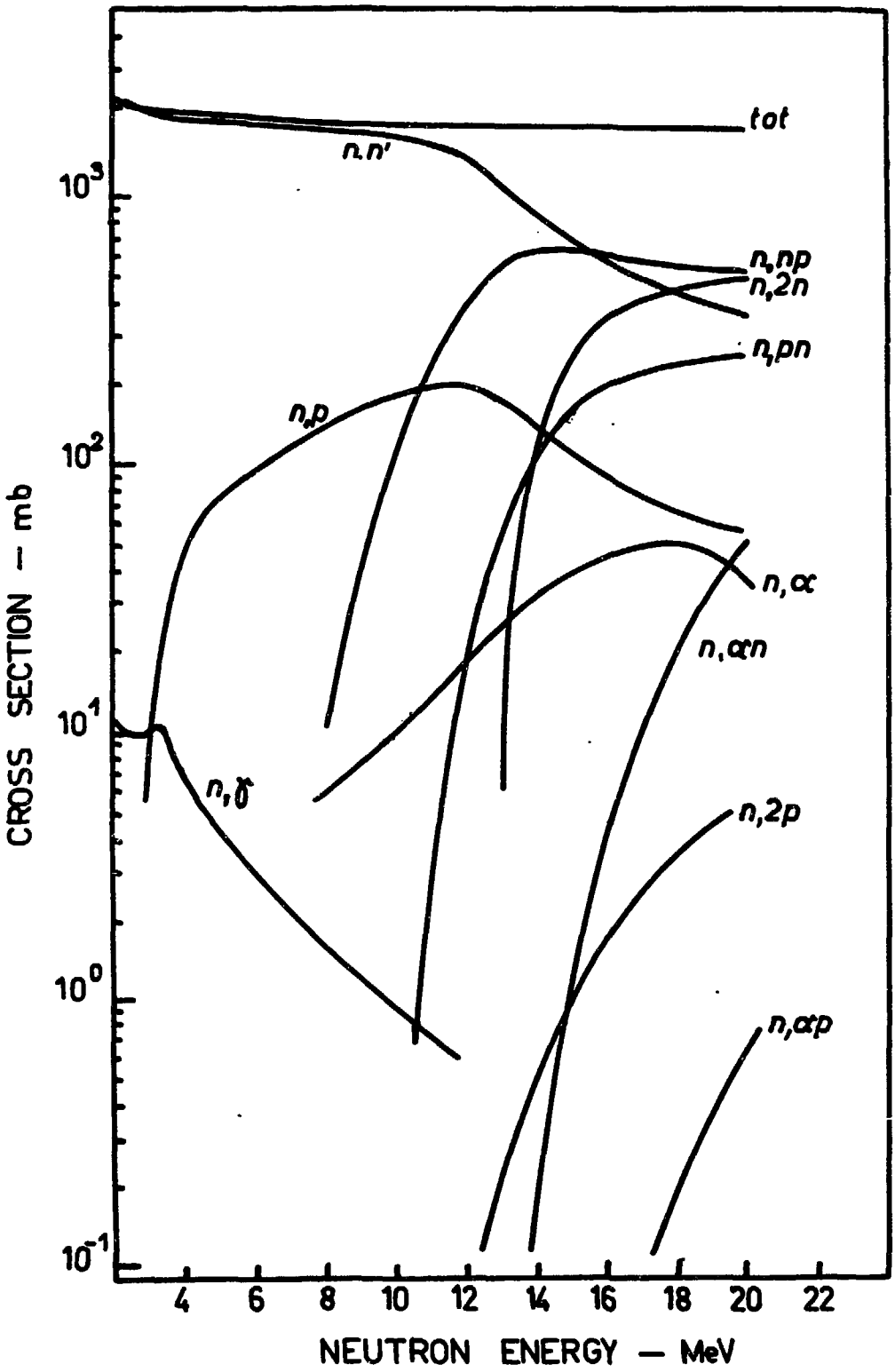

Fig. 6 Cross sections for fast neutron induced reactions on 92-Mo calculated with use of EMPIRE according to the Hauser-Feshbach and the geometry dependent hybrid models.

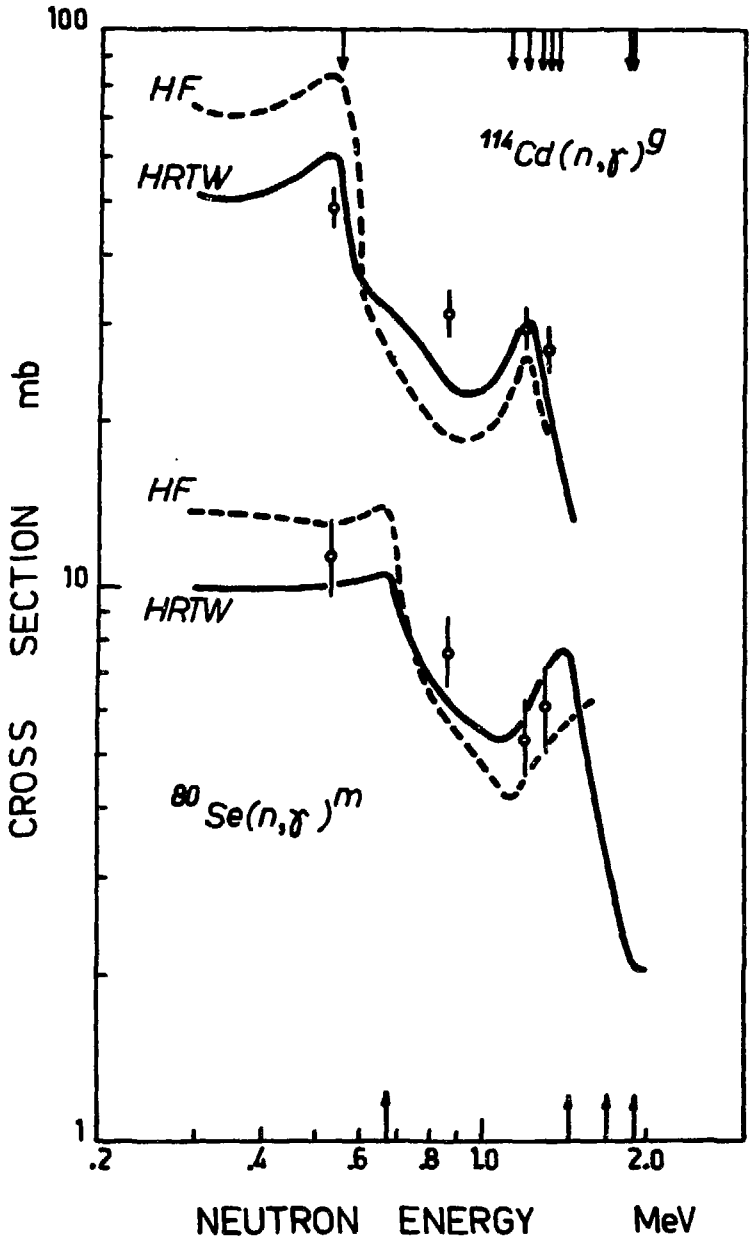

Fig. 7 Comparison of neutron capture cross sections calculated, with (HRTW) and without (HF) accounting for the width fluctuations, with experimental data obtained by the author. The arrows indicate positions of the excited levels of the target nuclei.

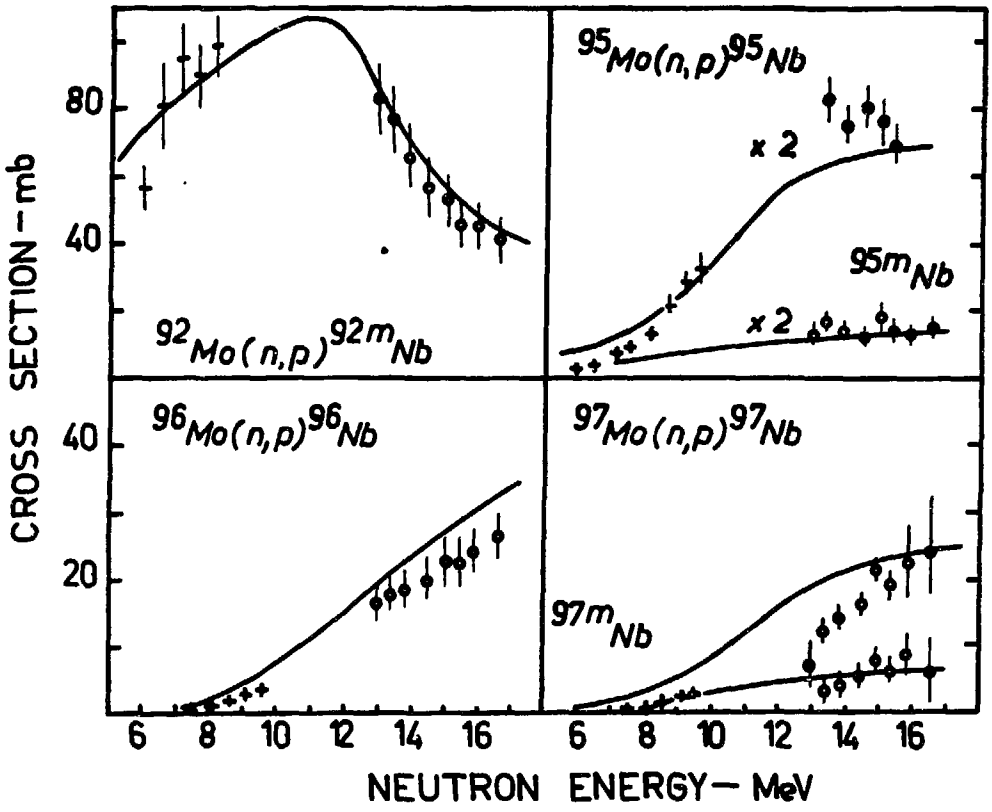

Fig. 6 Comparison of cross sections calculated for the (n,p) reaction on molybdenum isotopes with experiments: open circles - measurements of the author and crosses - data measured in the INCh at Jülich.

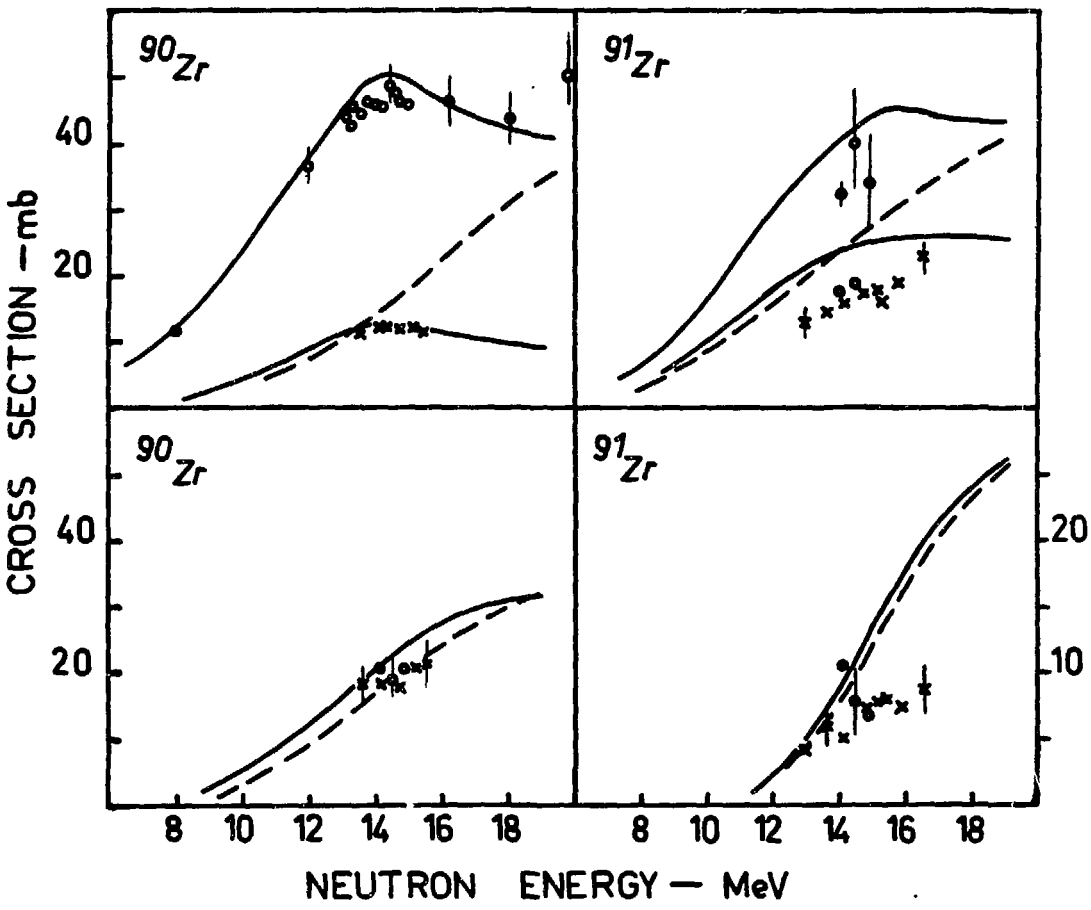

Fig. 9 Comparison of cross sections calculated for the (n,p) reaction on zirconium isotopes with experiments: open circles - data compiled from the Handbook on Nuclear Activation, IAEA Technical Report Series No 156, Vienna 1974, p. 87, crosses - measurements of the author.

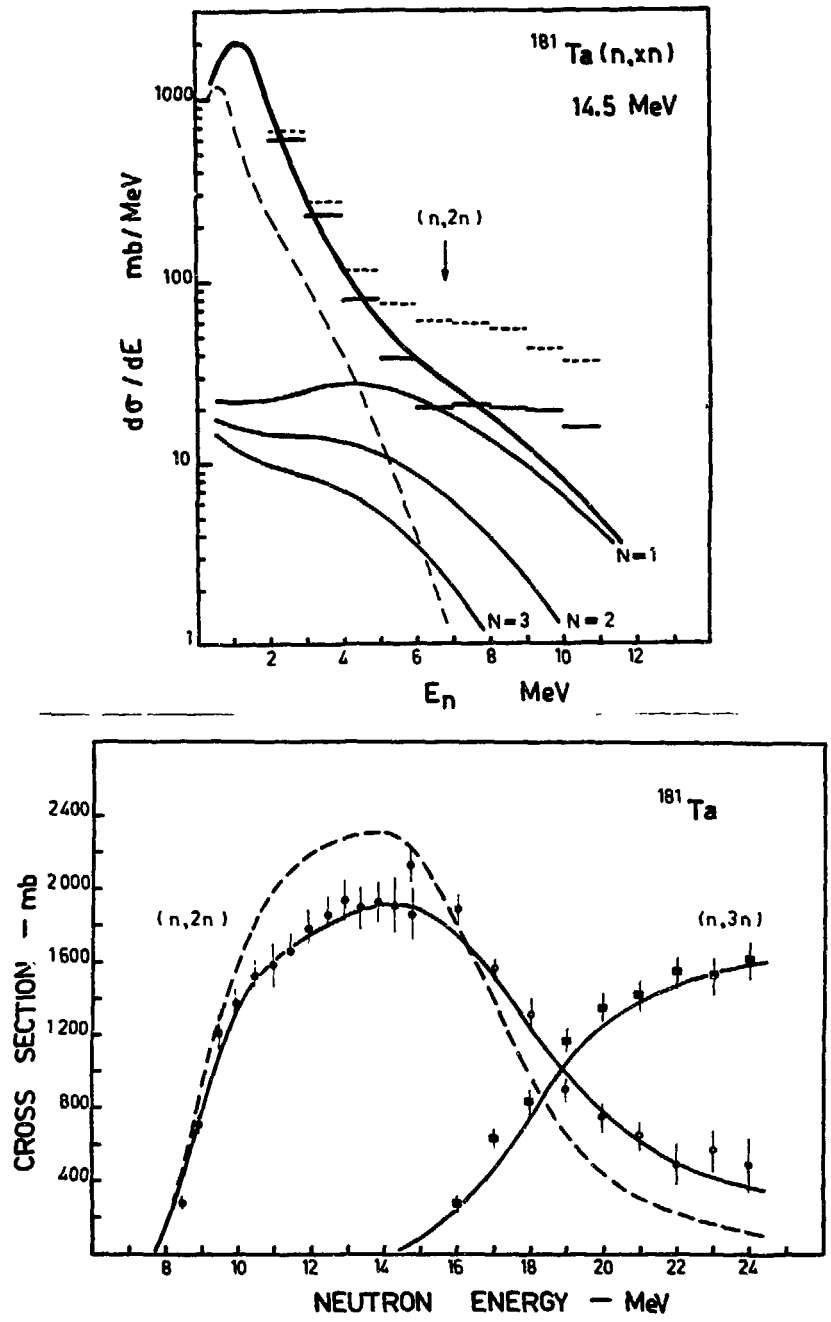

Figs. 10 - 11 Total neutron spectrum for the ^{181}Ta + n reaction at 14.5 MeV and the excitation curve for the ^{181}Ta(n,2n)^{180}Ta reaction (below) as calculated with EMPIRE's multi-step compound option for the pre-equilibrium emission (solid lines). The dashed lines correspond to the decay of the compound nucleus only. For details see ref. [29].

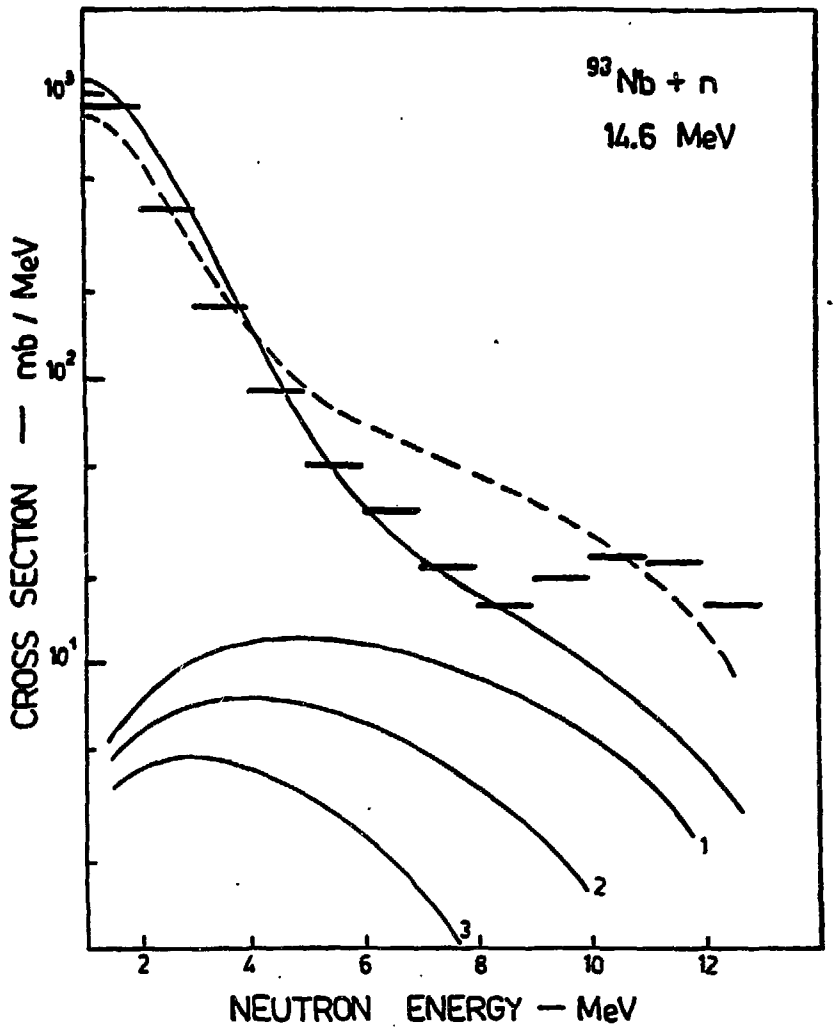

Fig. 12 Comparison of calculated (HF plus MSC) neutron spectrum with the symmetric portion of the angular distributions (horizontal bars) measured for the 93-Nb + n reaction at 14.6 MeV (Osaka University data). Solid line is with Ericson state densities and harmonic oscillator wave functions. Dashed line shows the effect of bound configurations.

Attachment

M. Herman, A. Marcinkowski, K. Stankiewictz "A program for calculation of spectra and cross sections within the combined pre-equilibrium/compound nucleus model of nuclear reactions". Comput. Phys. Commun. 33 p. 373-398 (1984). (Not microfiched)